Supporting Information

Influence of the Substitution Pattern of four Naphthalenedicarboxylic Acids on the Structures and Properties of Group 13 Metal-organic Frameworks and Coordination Polymers

By Timo Rabe,[a] Harm Pewe,[a] Helge Reinsch,[a] Tom Willhammar,[b] Erik Svensson Grape[b] and Norbert Stock*[a]

[a]Christian-Albrechts-Universität zu Kiel, 24118 Kiel, Max-Eyth-Straße 2

[b]Stockholm University, 10691 Stockholm, Frescativägen 8

1. Thermogravimetric measurement of $Ga(NO_3)_3 \cdot x\ H_2O$

In order to study the water content of $Ga(NO_3)_3 \cdot x\ H_2O$ thermogravimetric measurements were carried out resulting in seven water molecules per sum formula (Fig. S1). The residue after the thermogravimetric measurement of $Ga(NO_3)_3 \cdot x\ H_2O$ was studied by powder X-ray diffraction (PXRD) showing that crystalline *ß*-Ga_2O_3 had formed (Fig. S2). The device used for this measurement was a Lindseis STA PT 1000 (nitrogen flow = 8 dm^3/h, heating rate = 4K/min).

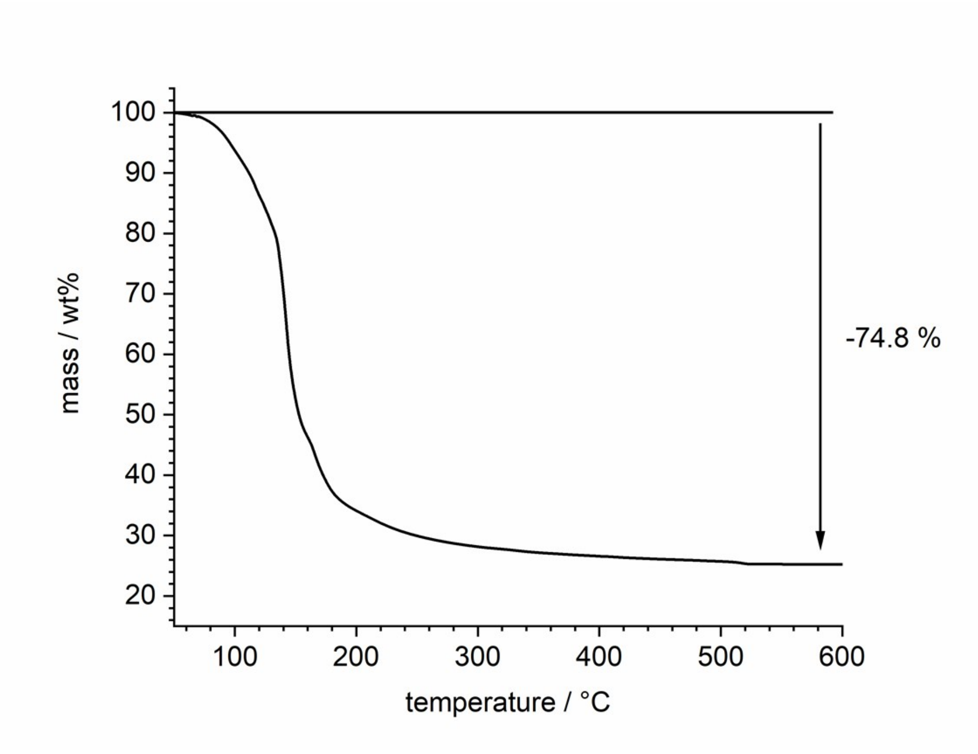

Figure S1: *Curve of the thermogravimetric measurement for* $Ga(NO_3)_3 \cdot x\ H_2O$.

Table S1: *Result of the thermogravimetric analysis for* $Ga(NO_3)_3 \cdot x\ H_2O$.

Product/Step	**calcd / %**	**obs / %**	**ΔT / °C**
$7\ H_2O$, 6 NO*	75.5	74.8	RT-160
Ga_2O_3	24.5	25.2	160-1000

*The measurement was carried out under a nitrogen flow and therefore it is anticipated that the remaining oxygen formed NO molecules.

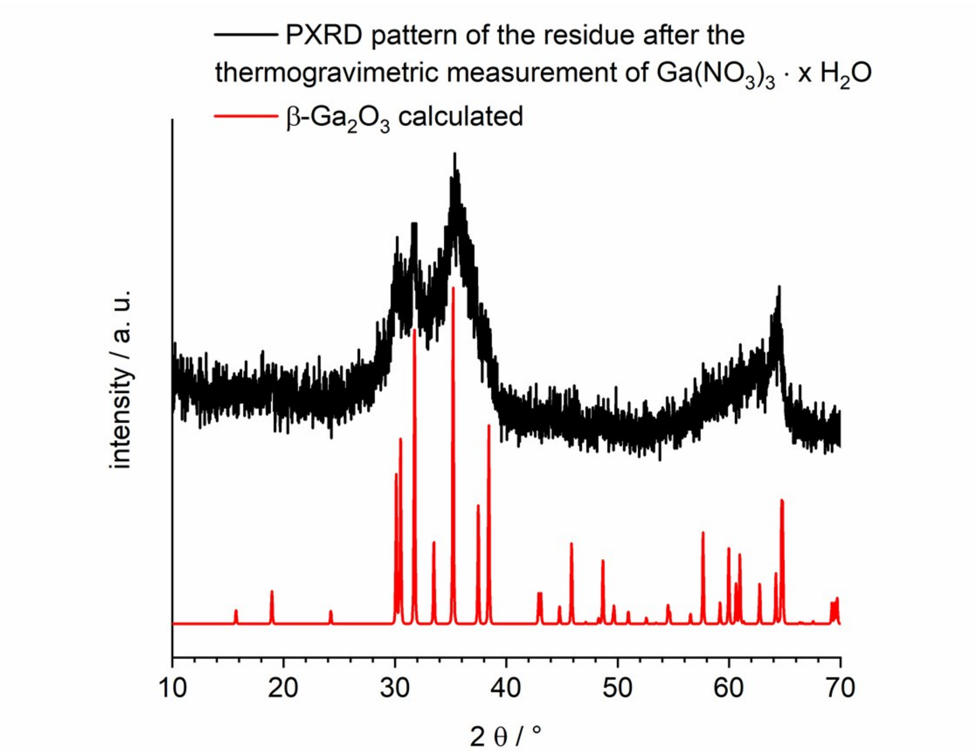

Figure S2: *PXRD pattern of the* $Ga(NO_3)_3 \cdot x\ H_2O$ *residue after the thermogravimetric measurement.*

2. Detailed syntheses procedures for [Ga(OH)(1,4-ndc)], [M(OH)(1,8-ndc)] and [$M_2(OH)_4$(2,3-ndc)] M = Al^{3+} or Ga^{3+} and [Ga(OH)(2,6-ndc)] and results of the CH-analysis of the reaction products

A 0.72 mol/l solution of $Ga(NO_3)_3 \cdot 7\ H_2O$ was used for all experiments.

The different molar ratios were found during our systematic investigation and represent the conditions at which the products of highest crystallinity could be obtained. The variations in molar ratios M : L for the optimized synthesis probably depend on several factors like solubility in the different solvents at different temperatures or pH value of the reaction mixture.

Synthesis of [Ga(OH)(1,4-ndc)]

[Ga(OH)(**1,4-ndc**)] was hydrothermally synthesized from a mixture of gallium nitrate heptahydrate used as 0.72 mol/l solution, 1,4-H_2ndc as a solid and sodium hydroxide used as 2 mol/l solution. The optimized reaction mixture contained: 1 ml gallium nitrate solution (0.72 mol/l) (7.2 mmol), 1,4-H_2ndc 130 mg (6.0 mmol), 0.3 ml NaOH solution (2 mol/l) (0.6 mmol) and water 8.7 ml (482.9 mmol). The synthesis was carried out under microwave-assisted heating in a 20 mL glass reactor at 140 °C for 4 h under stirring. After isolation by filtration the resulting light brown powder was redispersed under ultrasonication and subsequently centrifuged two times with 10 ml of *N,N'*-Dimethylformamide (*N,N'*-DMF) and two times with 10 ml ethanol. Afterwards the product was dried at 85 °C for 16 h. The pH-value of the reaction mixture was measured before (pH = 4) and after (pH = 6) heating. Elemental analysis: [Ga(OH)(**1,4-ndc**)] · 2 H_2O, C = 46.32 % (calcd 42.78 %), H = 3.39 % (cald 3.29 %).

Yield: 159 mg (73.6 % based on Ga^{3+}).

Synthesis of [Ga(OH)(1,8-ndc)] and [$Ga_2(OH)_4$(2,3-ndc)]

[Ga(OH)(**1,8-ndc**)] and [$Ga_2(OH)_4$(**2,3-ndc**)] were hydrothermally synthesized under nearly identical reaction conditions. The optimized reaction mixtures contained: 0.5 ml gallium nitrate solution (0.72 mol/l) (3.6 mmol), 108 mg 2,3-H_2ndc or 99 mg **1,8-ndc** anhydride (5 mmol), respectively, 0.5 ml NaOH solution (2 mol/l) (1 mmol) and 9 ml water (499.6 mmol). Reaction conditions and workup procedure were identical to the ones reported for [Ga(OH)(**1,4-ndc**)]. The pH-value for the reaction mixtures of [Ga(OH)(**1,8-ndc**)] was measured before (pH = 10) and after (pH = 6) heating, as well as the pH-value for the reaction mixture of [$Ga_2(OH)_4$(**2,3-ndc**)] before heating (pH = 6) and afterwards (pH = 6). Elemental analysis: [Ga(OH)(**1,8-ndc**)] C = 46.98 % (calcd 47.90 %), H = 2.24 % (calcd 2.99 %) and [$Ga_2(OH)_4$(**2,3-ndc**)] · H_2O, C = 33.39 % (calcd 32.78 %), H = 2.51 % (calcd 2.75 %).

[Ga(OH)(**1,8-ndc**)] Yield: 64 mg (58.3 % based on Ga^{3+}).

[Ga(OH)(**2,3-ndc**)] Yield: 65 mg (41.7 % based on Ga^{3+}).

Synthesis of [Ga(OH)(2,6-ndc)]

[Ga(OH)(**2,6-ndc**)] was synthesized under solvothermal reaction conditions in methanol as the solvent. A typical reaction mixture contained 0.5 ml gallium nitrate solution (0.72 mol/l) (4.3 mmol), 108 mg 2,6-H_2ndc (5 mmol), 0.6 ml NaOH solution (2 mol/l) (1.2 mmol) and 8.9 ml methanol (219.45 mmol). The reaction temperature was set to 150 °C for 4 h. Reaction conditions and workup procedure were identical to the ones reported for [Ga(OH)(**1,4-ndc**)]. Elemental analysis: [Ga(OH)(**2,6-ndc**)] · H_2O, C = 42.68 % (calcd 45.19 %), H = 2.56 % (calcd 2.84 %). The differences of the carbon value indicates the contamination of the sample with small amounts of presumably amorphous gallium oxide, which was also confirmed by thermogravimetric measurements (see below).

[Ga(OH)(**2,6-ndc**)] Yield: 97 mg (74.4 % based on Ga^{3+}).

Synthesis of [Al(OH)(1,8-ndc)]

[Al(OH)(**1,8-ndc**)] was synthesized in a 2 ml Teflon reactor under solvothermal reaction conditions employing a reaction mixture, which contained 50 µl aluminum nitrate solution (1 mol/l) (50.0 µmol), 9.9 mg 1,8-naphthalenedicarboxylic anhydride (45.4 µmol), 940 µl water (52.3 µmol) and 10 µl NaOH solution (2 mol/l) (0.02 mmol). After sealing the steel autoclave it was heated to 160 °C within 1 h. The temperature was held for 36 h and cooled down to room temperature in 5 h. The pH-value of the reaction mixture was measured before (pH = 6) and after (pH = 6) heating. Afterwards the product was isolated by filtration and washed two times with 50 ml of *N,N'*-DMF and two times with ethanol. Elemental analysis: [Al(OH)(**1,8-ndc**)], C = 55.2 % (calcd 55.8 %), H = 2.7 % (calcd 2.7 %).

[Al(OH)(**1,8-ndc**)] Yield: 4.5 mg (28.0 % based on Al^{3+}).

Synthesis of [$Al_2(OH)_4$(2,3-ndc)]

[$Al_2(OH)_4$(**2,3-ndc**)] · H_2O was synthesized in a 20 ml Teflon reactor from a reaction mixture containing 1.45 ml aluminum sulphate solution (0.5 mol/l) (0.7 mmol), 313 mg 2,3-naphthalenedicarboxylic acid (1.5 mmol), 3.44 ml water (191.2 mmol), 6 ml *N,N'*-DMF (78.0 mmol) and 1.12 ml concentrated acetic acid (19.6 mmol). The sealed autoclave was heated to 120 °C within 1 h. This temperature was held for 12 h and cooled down to room temperature in 5 h. The product was isolated by filtration and washed with 50 ml of water and acetone. Elemental analysis: [$Al_2(OH)_4$(**2,3-ndc**)] · H_2O, C = 39.8 % (calcd 40.7 %), H = 3.3 % (calcd 3.3 %).

[$Al_2(OH)_4$(**2,3-ndc**)] Yield: 60 mg (21.4 % based on Al^{3+}).

3. Transmission electron diffraction (TEM) measurement

The sample was crushed in an agate mortar, dispersed in absolute ethanol. Then, a droplet of the suspension was transferred onto a copper grid covered by a holey carbon film. The grid was mounted to a single-tilt holder. The electron diffraction data were collected using a JEOL JEM-2100 transmission electron microscope (TEM) operated at an accelerating voltage of 200 kV. The continuous rotation electron diffraction (cRED) data were collected by continuously tilting the goniometer with a tilt speed of 0.45 °/s. During tilting the crystal was tracked by sequential defocusing of the intermediate lens using the software Instamatic.[1] The diffraction patterns were collected using the high-speed hybrid detection camera Timepix Quad (ASI). The datasets were processed using X-ray Detector Software (XDS)[2] in order to extract intensities for structure solution and refinement. The structure was solved using the software SHELX[3] and the least-squares refinement was done in SHELXL-97[4] using atomic scattering factors for electrons extracted from SIR2014 (Tab. S2).[5]

Table S2: *Details of the electron diffraction data and refinement.*

Parameter	**Value**
Crystal system	Tetragonal
Space group	$P4_2/nmc$ (No. 137)
a, Å	21.57
b, Å	21.57
c, Å	6.70
α, °	90
β, °	90
γ, °	90
Volume, Å^3	3117.27
λ, Å	0.0251
Exposure time per frame (s)	0.6
Tilt range, °	-52.2 - +62.3
Resolution, Å	0.80
Completeness, %	88.6
R_{int}	0.1637
R1	0.2483
No. of symmetry independent reflections	1685

4. Rietveld refinements, asymmetric units and bond lengths

All indexing and refinement steps of the PXRD patterns described herein was carried out using TOPAS academics.[6] Where necessary, the software used for structural modelling and optimization by force-field calculations was Materials Studio.[7]

[Ga(OH)(1,4-ndc)]

The crystal structure model as determined from electron diffraction data was first optimized by force-field calculations and subsequently refined by the Rietveld method. Residual electron density inside the pores was identified by Fourier synthesis and attributed to partially occupied oxygen atoms, which serve as placeholders for guest molecules like water. The carbon atoms of the aromatic fragment of the linker molecule were treated as rigid body, hence no standard deviation is given. All other atoms were freely refined using only distance restrains and element specific temperature factors. The final plot is shown in Fig. S3 along with the asymmetric unit in Fig. S4 and some relevant bond distances in Tab. S3.

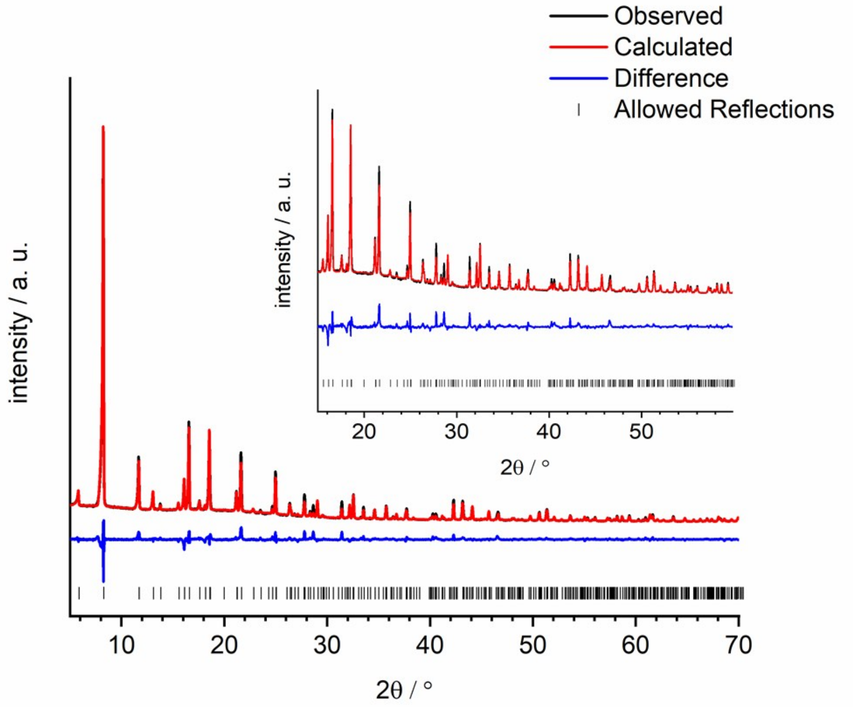

*Figure S3: Final plot of the Rietveld refinement for [Ga(OH)(**1,4-ndc**)]. The observed curve in black, the calculated curve in red, the difference curve in blue and the positions of allowed reflections as black lines.*

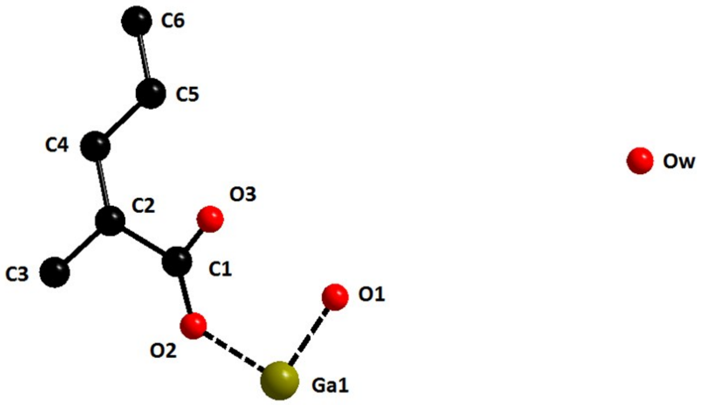

Figure S4: *Asymmetric unit of [Ga(OH)(**1,4-ndc**)].*

Table S3: *Selected atoms and bond lengths for [Ga(OH)(**1,4-ndc**)].*

Atom #1	Atom #2	bond lengths / Å
Ga1	O1	1.879(5)
	O2	1.93(2)
	O3	1.96(2)
C1	O3	1.26(4)
	O2	1.26(4)
	C2	1.55(2)
C2	C3	1.405
	C4	1.426
C4	C5	1.415
C5	C6	1.395

[Ga(OH)(1,8-ndc)]

The crystal structure of Ga-MIL-122[8] [$M_2(OH)_2(C_{14}O_8H_4)$] (M = Al^{3+}, Ga^{3+}, In^{3+}) was used as starting model. The originally present linker molecules (1,4,5,8-naphthalenetetracarboxylate) were "cut" in half and manipulated into two separate 1,8-naphthalenedicarboxylate ions. Subsequently the symmetry ($P2_1/c$) was lowered to $P1$ and the cell parameters (a = 9.6501(1), b = 10.0585(1), c = 6.75069(9) Å, β = 92.4786(9)°) were set to the corresponding indexed lattice parameter values for a different monoclinic setting (a = 17.059(2), b = 10.039(3), c = 6.719(2) Å, α = β = 90°, γ = 116.24(2)°). This model was optimized by force-field calculations and exhibited $P2_1/c$ symmetry (with changed cell setting), as also suggested by indexing. The model was thus subsequently refined by the Rietveld method. The carbon atoms of the aromatic part of the linker molecule were treated as rigid body, hence no standard deviation is given. All other atoms were freely refined using only distance restraints and one overall temperature factor. To account for preferred orientation and peak broadening, a 4th order spherical harmonics function was used. The final Rietveld plot is shown below in Fig. S5 along with the asymmetric unit in Fig. S6 and some relevant bond distances in Tab. S4.

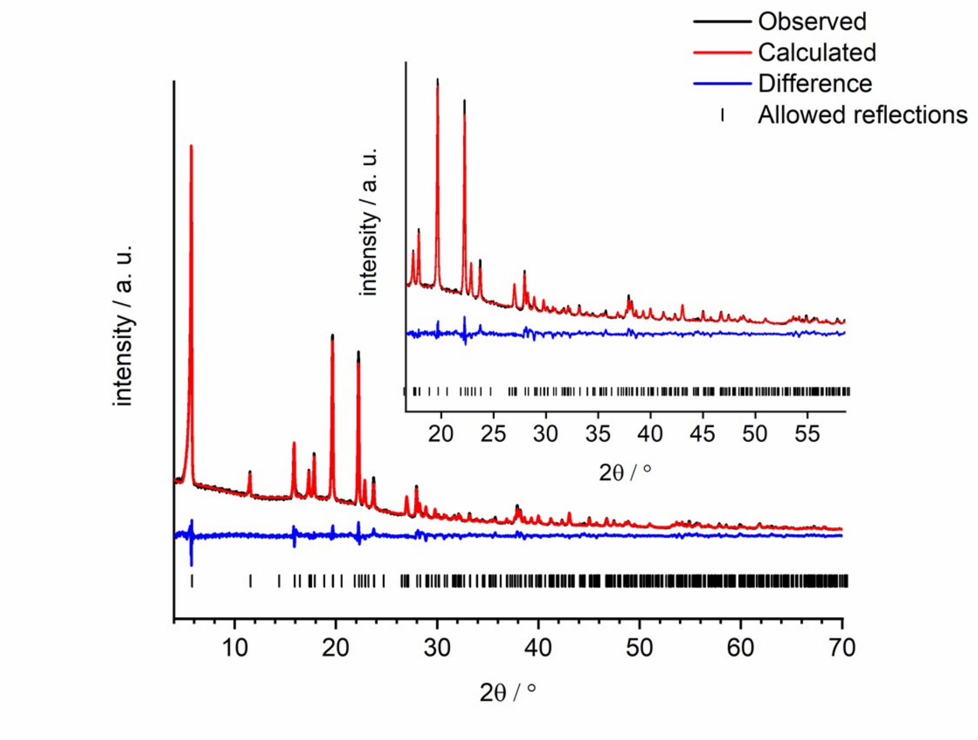

Figure S5: *Final plot of the Rietveld refinement for [Ga(OH)(**1,8-ndc**)]. The observed curve in black, the calculated curve in red, the difference curve in blue and the positions of allowed reflections as black lines.*

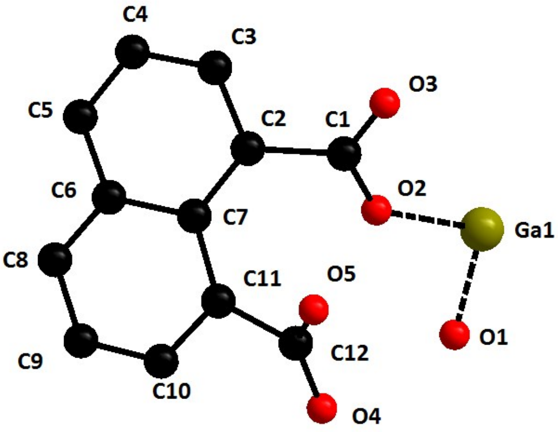

Figure S6: *Asymmetric unit of [Ga(OH)(**1,8-ndc**)].*

Table S4: *Selected atoms and bond lengths for [Ga(OH)(**1,8-ndc**)]. The slightly different C-C values of the aromatic ring is a result from the force field calculations that were performed to set up the structure model and the fact that this part of the structure was refined as a rigid body.*

Atom #1	Atom #2	bond lengths / Å
Ga1	O1	1.82(3)
	O2	2.05(5)
	O3	2.00(6)
	O4	1.97(3)
	O5	1.98(3)
C1	O3	1.27(7)
	O2	1.30(6)
	C2	1.56(5)
C12	O5	1.28(6)
	O4	1.30(7)
	C11	2.42(5)
C2	C3	1.416
	C7	1.429
C3	C4	1.387
C5	C6	1.386
	C4	1.397
C6	C8	1.392
	C7	1.445
C7	C2	1.429
	C11	1.431
C8	C9	1.380
	C6	1.392
C10	C9	1.382
	C11	1.408
C11	C12	1.553

[Ga(OH)(2,3-ndc)]

The pattern could be indexed in a monoclinic unit cell with possible space group symmetry *P*2/*c*, thus being closely related to the crystal structure of CAU-15[9] with elongated cell parameters a = 6.919(4), b = 12.751(4), c = 9.722(4) Å, β = 127.51(3)°). Thus the crystal structure of CAU-15 was used as starting model for force-field calculations. The indexed unit cell parameters were imposed, the linker molecules extended from phthalate to naphthalenedicarboxylate and the metal ions were changed. Subsequently the optimized model was refined by the Rietveld method. Residual electron density between the layers was identified by Fourier synthesis and attributed to partially occupied oxygen atoms, which serve as placeholders for guest molecules like water. A subtle preferred orientation along (11-2) was taken into account and all atoms were freely refined using only distance restrains and element specific temperature factors. The final plot is shown below Fig. S7 along with the asymmetric unit Fig. S8 and some relevant bond distances Tab. S5.

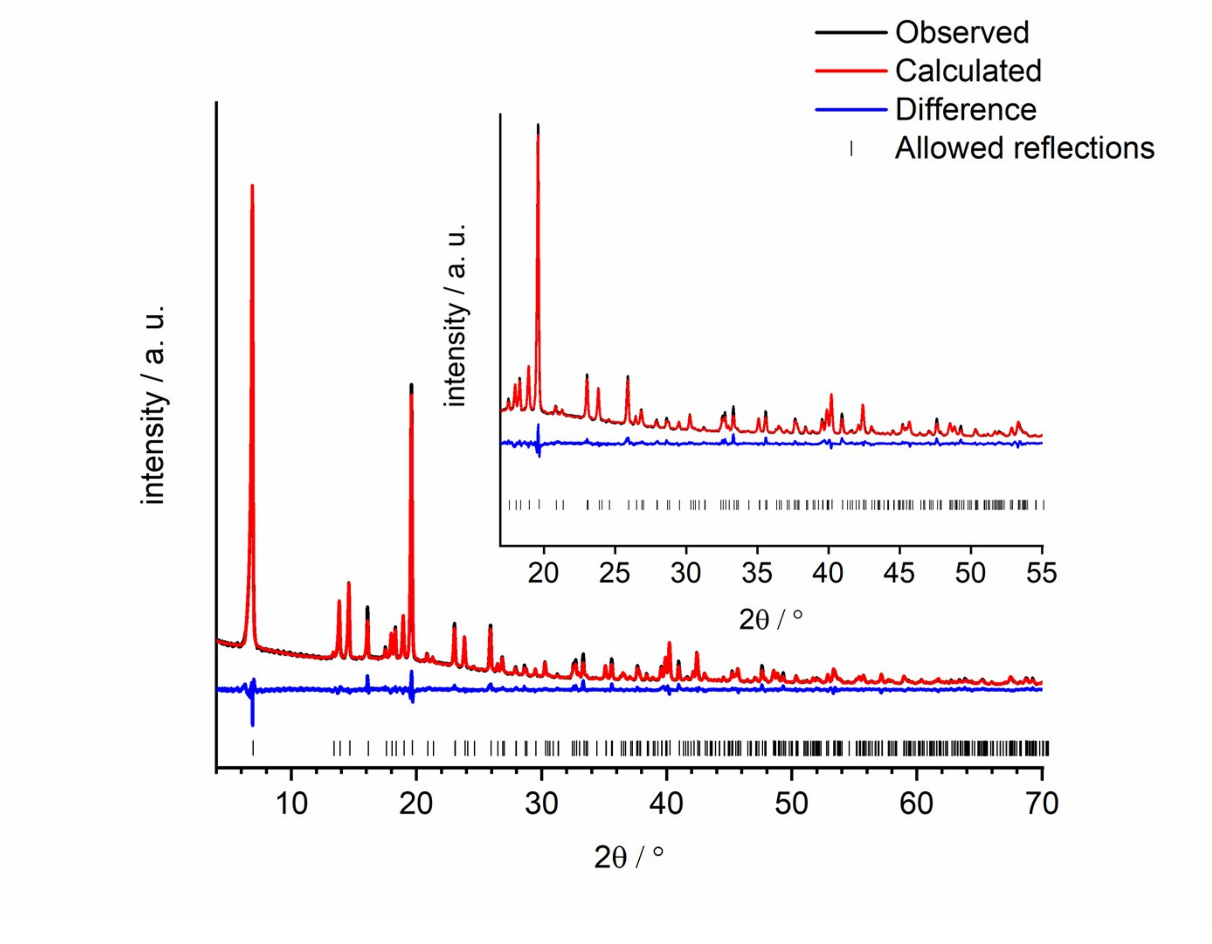

Figure S7: *Final plot of the Rietveld refinement for [Ga$_2$(OH)$_4$(**2,3-ndc**)]. The observed curve in black, the calculated curve in red, the difference curve in blue and the positions of allowed reflections as black lines.*

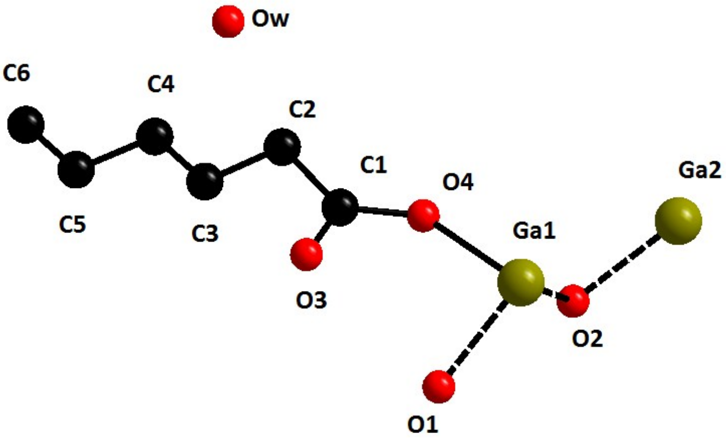

Figure S8: *Asymmetric unit of [Ga(OH)(**2,3-ndc**)].*

Table S5: *Selected atoms and bond lengths for [Ga(OH)(**2,3-ndc**)].*

Atom #1	Atom #2	bond lengths / Å
Ga1	O4	1.98(1)
	O2	1.98(1)
	O1	1.99(1)
Ga2	O1	2.00(1)
	O2	2.02(1)
	O3	1.98(1)
C1	O3	1.24(2)
	O4	1.28(2)
	C2	1.52(3)
C2	C3	1.36(2)
C4	C5	1.37(2)
C5	C6	1.37(2)

[Ga(OH)(2,6-ndc)]

The crystal structure of MIL-69[10] could be directly used as starting model for the Rietveld refinement after replacement of the metal ions. Residual electron density inside the pores was identified by Fourier synthesis and attributed to partially occupied oxygen atoms, which serve as placeholders for guest molecules like water. The carbon atoms of the aromatic fragment of the linker molecule were treated as rigid body, hence no standard deviations are given. All other atoms were freely refined using only distance restraints and element specific temperature factors. In addition a strong preferred orientation along (010) was also taken into account. The final plot is shown below Fig. S9 along with the asymmetric unit Fig. S10 and some relevant bond distances Tab. S6. Please note that no standard deviations are given for fragments refined as rigid bodies.

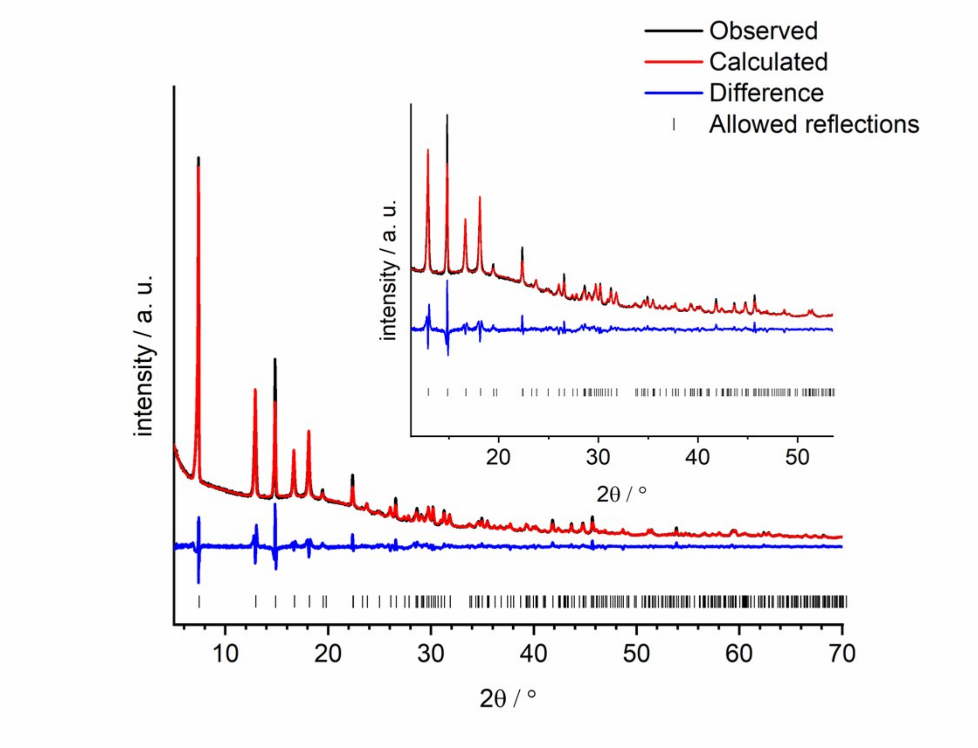

Figure S9: *Final plot of the Rietveld refinement for [Ga(OH)(**2,6-ndc**)]. The observed curve in black, the calculated curve in red, the difference curve in blue and the positions of allowed reflections as black lines.*

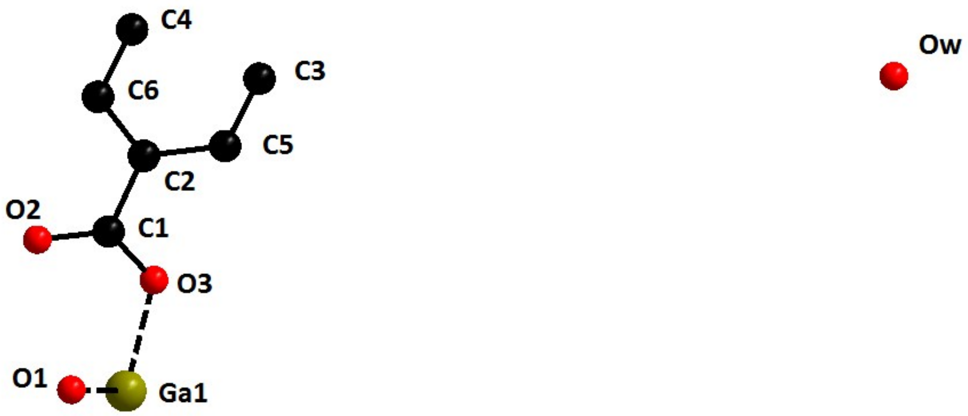

Figure S10: *Asymmetric unit of [Ga(OH)(**2,6-ndc**)].*

Table S6: *Selected atoms and bond lengths for [Ga(OH)(**2,6-ndc**)]. The slightly different C-C values of the aromatic ring is a result from the force field calculations that were performed to set up the structure model and the fact that this part of the structure was refined as a rigid body.*

Atom #1	Atom #2	bond lengths / Å
Ga1	O1	1.92(1)
	O2	1.96(2)
	O3	1.99(1)
C1	O2	1.25(1)
	O3	1.26(1)
	C2	1.49(1)
C2	C6	1.405
	C5	1.413
C3	C4	1.376
	C5	1.409
C4	C6	1.406

[Al(OH)(1,8-ndc)]

For the Rietveld refinement, the refined structure of the Ga-analogue was used as starting point. The linker molecule was treated as a rigid body and all other atoms were freely refined using only distance restraints with one overall temperature factor. The final plot is shown below (Fig. S11) along with the asymmetric unit (Fig. S12) and some relevant bond distances (Tab. S7). Please note that no standard deviations are given for fragments refined as rigid bodies.

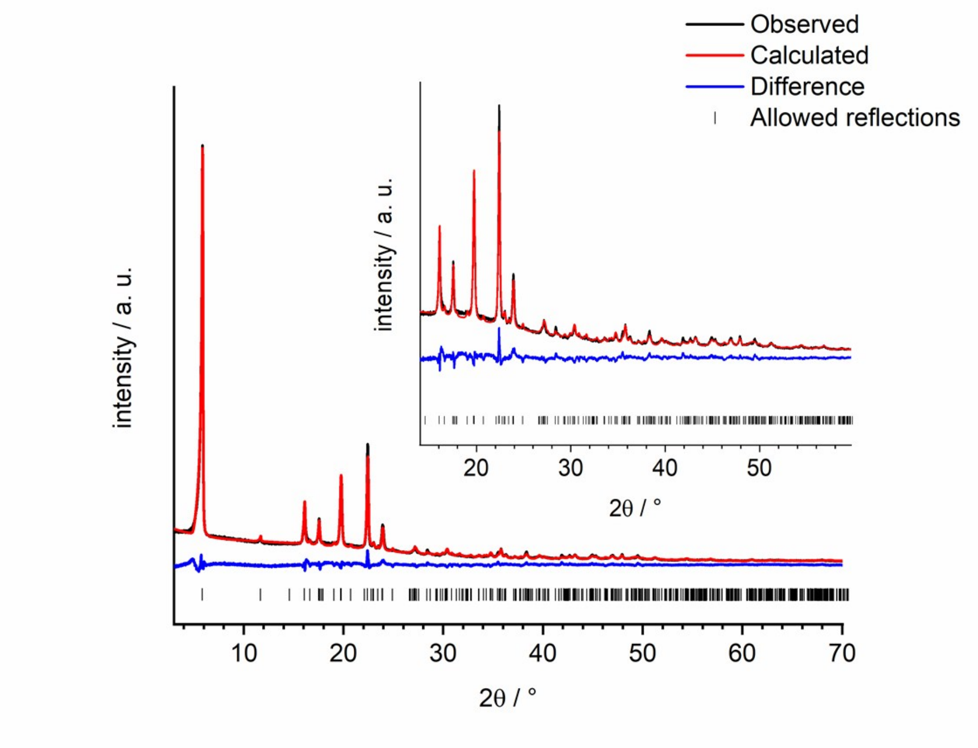

Figure S11: *Final plot of the Rietveld refinement for [Al(OH)(**1,8-ndc**)]. The observed curve in black, the calculated curve in red, the difference curve in blue and the positions of allowed reflections as black lines.*

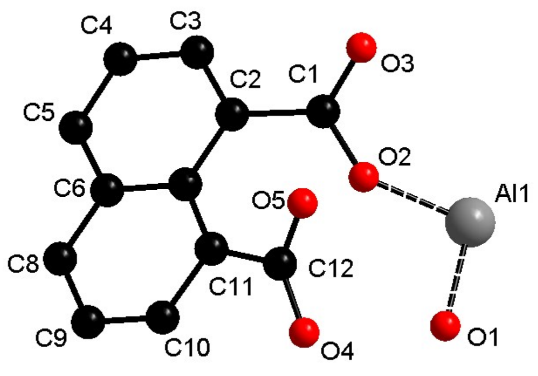

Figure S12: *Asymmetric unit of [Al(OH)(**1,8-ndc**)].*

Table S7: *Selected atoms and bond lengths for [Al(OH)(**1,8-ndc**)]. The slightly different C-C values of the aromatic ring is a result from the force field calculations that were performed to set up the structure model and the fact that this part of the structure was refined as a rigid body.*

Atom #1	Atom #2	bond lengths / Å
Al1	O1	1.86(4)
	O4	1.83(3)
	O5	1.94(2)
	O2	1.96(4)
	O3	1.88(4)
C1	O3	1.29(5)
	O2	1.27(5)
	C2	1.51(4)
C12	O5	1.23(5)
	O4	1.22(5)
	C11	1.54(3)
C2	C3	1.402
	C7	1.423
C3	C4	1.377
C5	C6	1.389
	C4	1.373
C6	C8	1.388
	C7	1.432
C7	C2	1.423
	C11	1.423
C8	C9	1.372
	C6	1.388
C10	C9	1.378
	C11	1.401
C11	C12	1.550

[$Al_2(OH)_4$(2,3-ndc)]

For the Rietveld refinement, the crystal structure of the Ga-analogue was used as starting point. The linker molecule was treated as a rigid body and all other atoms were freely refined using only distance restraints with one overall temperature factor. The final plot is shown below (Fig. S13) along with the asymmetric unit (Fig. S14) and some relevant bond distances (Tab. S8). Please note that no standard deviations are given for fragments refined as rigid bodies.

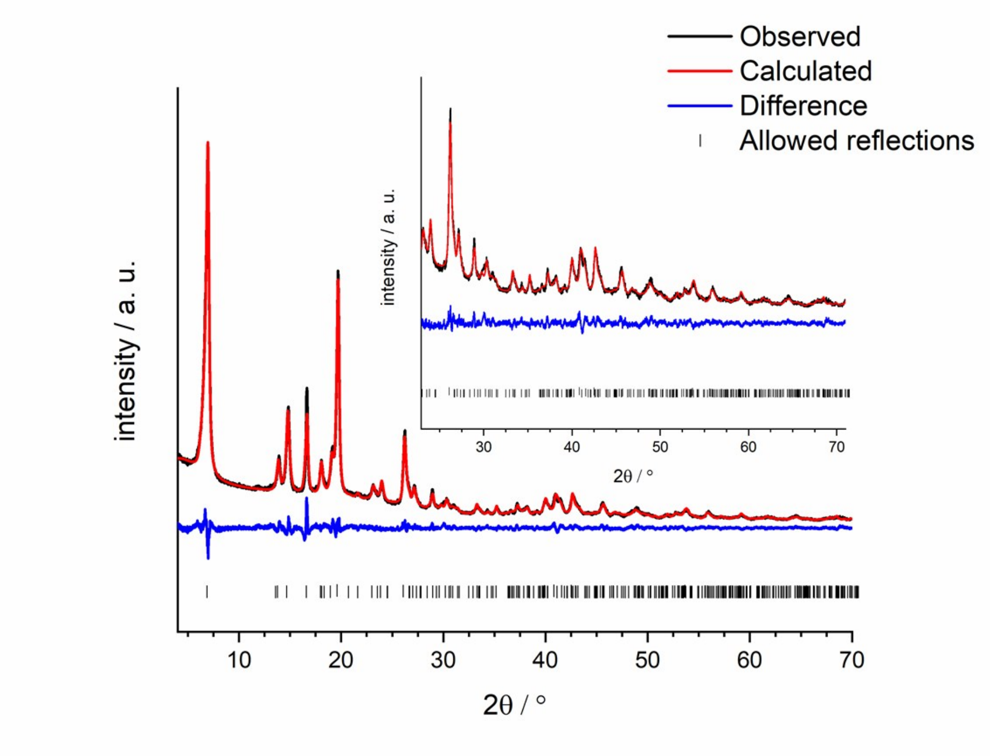

Figure S13: *Final plot of the Rietveld refinement for [$Al_2(OH)_4$(**2,3-ndc**)]. The observed curve in black, the calculated curve in red, the difference curve in blue and the positions of allowed reflections as black lines.*

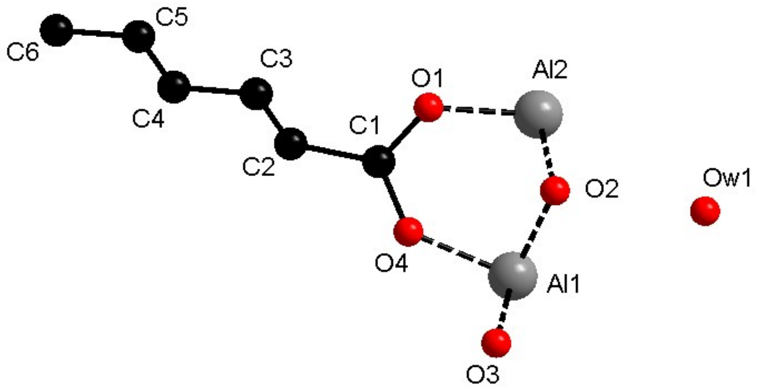

Figure S14: *Asymmetric unit of [$Al_2(OH)_4$(**2,3-ndc**)].*

Table S8: *Selected atoms and bond lengths for [$Al_2(OH)_4$(**2,3-ndc**)]. The slightly different C-C values of the aromatic ring is a result from the force field calculations that were performed to set up the structure model and the fact that this part of the structure was refined as a rigid body.*

Atom #1	Atom #2	bond lengths / Å
Al1	O2	1.85(9)
	O3	1.89(2)
	O4	1.93(2)
Al2	O1	1.92(3)
	O2	1.94(2)
	O3	1.88(9)
C1	O1	1.26(4)
	O4	1.30(2)
	C2	1.51(4)
C2	C3	1.383
C4	C5	1.404
	C3	1.397
C5	C6	1.391

5. IR-spectroscopy

IR-spectra of all compounds were collected on a Bruker ALPHA-FT-IR A220/D-01 using an ATR-unit and are shown in Fig. S15-20.

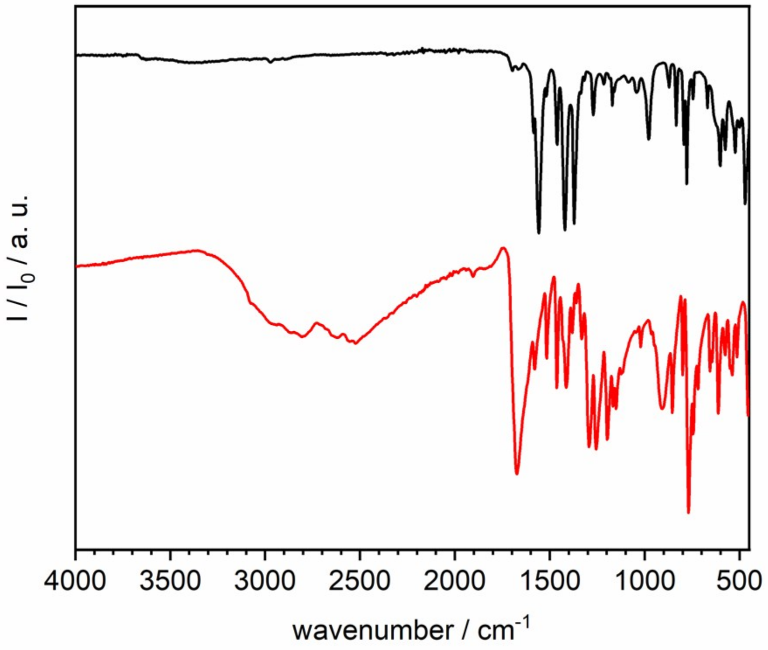

Figure S15: *IR-spectra of [Ga(OH)(**1,4-ndc**)] (black) and **$H_2$1,4-ndc** (red) in comparison.*

Table S9: *Assignment the vibrational bands in the IR-spectra of [Ga(OH)(**1,4-ndc**)].*[11]

Functional group	**Intensity**	**Observed value / cm^{-1}**	**Vibration**
-C-H	s-vs	871	κ(-H) out of plane
-C=O	w	1376	ν(-C=O) symmetric stretch
-C=C-	m	1511	ν(-C=C-) stretch
-C=O	s	1557	ν(-C=O) antisymmetric stretch
-OH	w	3361	ν(-OH) stretch

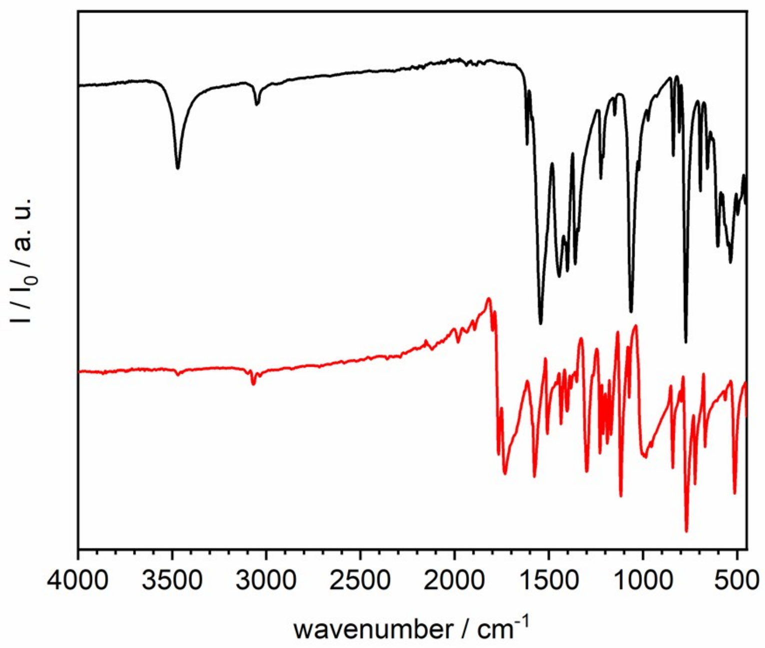

Figure S16: *IR-spectra of [Ga(OH)(**1,8-ndc**)] (black) and naphthalene-1,8-dicarboxylic anhydride (red) in comparison.*

Table S10: *Assignment of the vibrational bands in the IR-spectra of [Ga(OH)(**1,8-ndc**)].*[11]

Functional group	**Intensity**	**Observed value / cm^{-1}**	**Vibration**
-C=O	w	1360	ν(-C=O) symmetric stretch.
-C=O	s	1511	ν(-C=O) antisymmetric stretch.
-C=C-	m	1594	ν(-C=C-) char. naphthalene stretch.
=C-H	w-m	3048	ν(=C-H) stretch.
-OH	m-s	3474	ν(-OH) Hydrogen bonded, stretch.

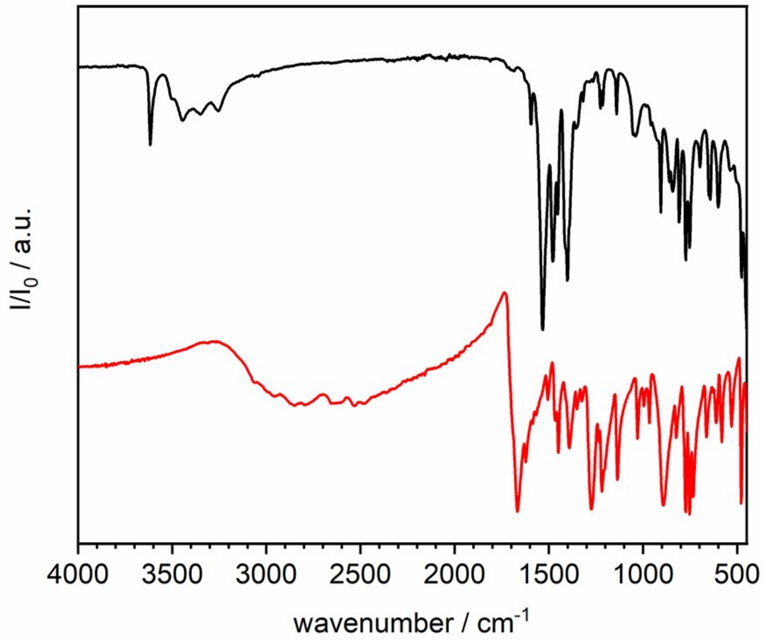

Figure S17: *IR-spectra of [Ga$_2$(OH)$_4$(**2,3-ndc**)] (black) and **H$_2$2,3-ndc** (red) in comparison.*

Table S11: *Assignment of the vibrational bands in the IR-spectra of [Ga$_2$(OH)$_4$(**2,3-ndc**)].*[11]

Functional group	**Intensity**	**Observed value / cm^{-1}**	**Vibration**
-C-H	s-vs	812	κ(-H) out of plane
-C=O	w	1391	ν(-C=O) symmetric stretch
-C=C-	m	1478	ν(-C=C-) stretch
-C=O	s	1535	ν(-C=O) antisymmetric stretch
-C-H	w	3044	ν(-C-H) stretch
-OH	m-s	3636	ν(-OH) stretch

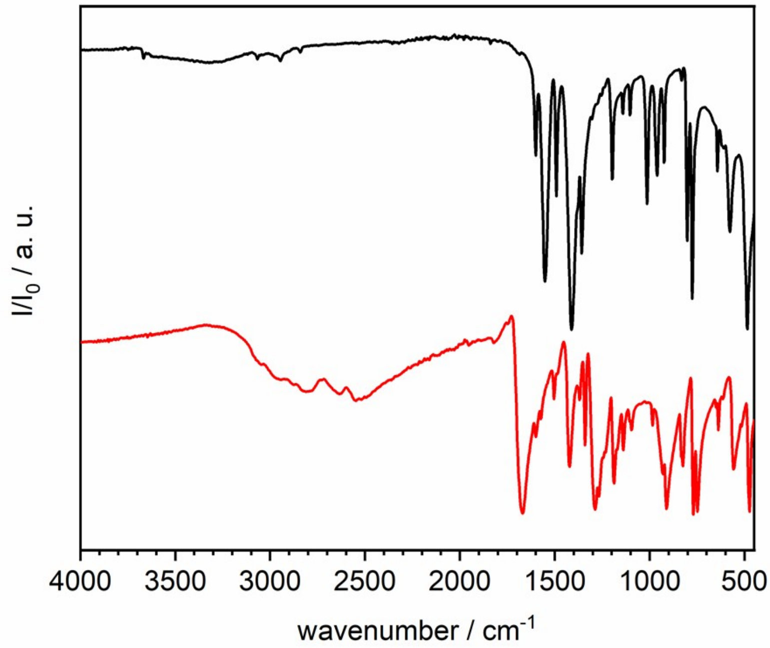

Figure S18: *IR-spectra of [Ga(OH)(**2,6-ndc**)] (black) and **$H_2$2,6-ndc** (red) in comparison.*

Table S12: *Assignment of the vibrational bands in the IR-spectra of [Ga(OH)(**2,6-ndc**)].*[11]

Functional group	**Intensity**	**Observed value / cm^{-1}**	**Vibration**
-C=O	w	1410	ν(-C=O) symmetric stretch.
-C=C-	m	1550	ν(-C=C-) char. naphthalene stretch.
-C=O	s	1602	ν(-C=O) antisymmetric stretch.
-C-H	w	3070	ν(=C-H) stretch.
-OH	w	3670	ν(-OH) Hydrogen bonded, stretch.

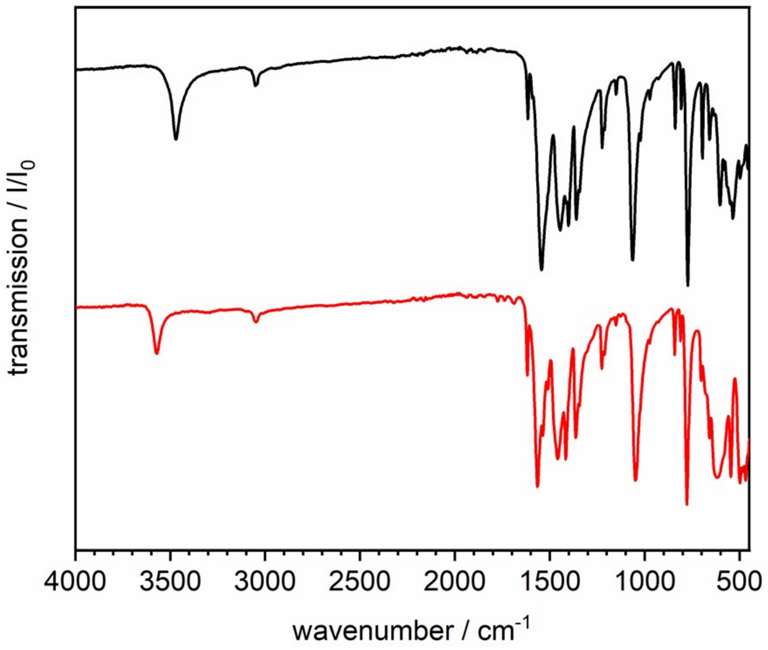

Figure S19: *IR-spectra of [Ga(OH)(**1,8-ndc**)] (black) and [Al(OH)(**1,8-ndc**)] (red) in comparison.*

Table S13: *Assignment of the vibrational bands in the IR-spectra of [Ga(OH)(**1,8-ndc**)] and [Al(OH)(**1,8-ndc**)].*[11]

Functional group	Intensity	Observed value [Ga(OH)(1,8-ndc)] / cm^{-1}	Observed value [Al(OH)(1,8-ndc)] / cm^{-1}	Vibration
-C=O	w	1360	1360	ν(-C=O) symmetric stretch.
-C=O	s	1515	1539	ν(-C=O) antisymmetric stretch.
-C=C-	m	1594	1564	ν(-C=C-) char. naphthalene stretch.
=C-H		3048	3048	ν(=C-H) stretch.
-OH	m-s	3474	3575	ν(-OH) Hydrogen bonded, stretch.

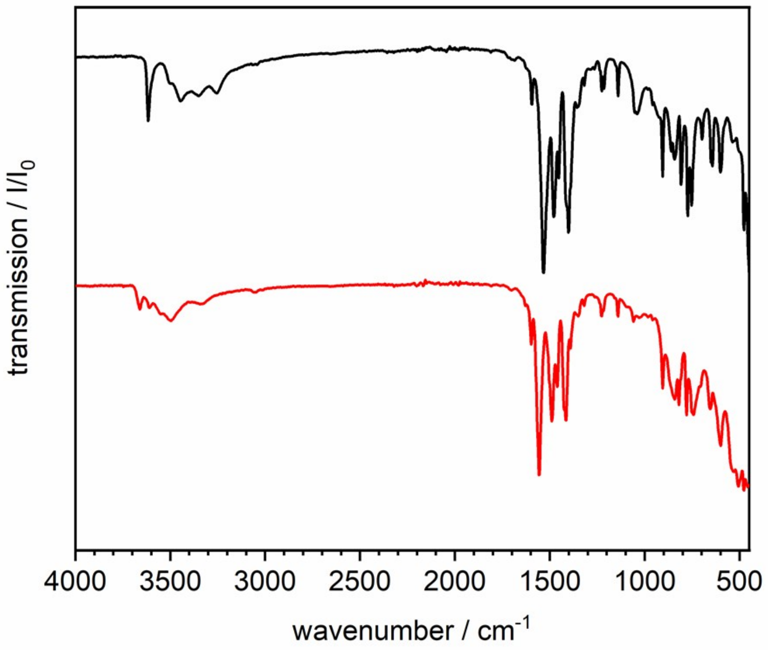

Figure S20: *IR-spectra of [$Ga_2(OH)_4$(**2,3-ndc**)] (black) and [$Al_2(OH)_4$(**2,3-ndc**)] (red) in comparison.*

Table S14: *Assignment of the vibrational bands in the IR-spectra of [$Ga_2(OH)_4$(**2,3-ndc**)] and [$Al_2(OH)_4$(**2,3-ndc**].*[11]

Functional group	**Intensity**	**Observed value [$Ga_2(OH)_4$(2,3-ndc)] / cm^{-1}**	**Observed value [$Al_2(OH)_4$(2,3-ndc)] / cm^{-1}**	**Vibration**
-C-H	s-vs	812	819	κ(-H) out of plane
-C=O	w	1391	1391	ν(-C=O) symmetric stretch
-C=C-	m	1478	1491	ν(-C=C-) stretch
-C=O	s	1535	1554	ν(-C=O) antisymmetric stretch
-C-H	w	3044	3051	ν(-C-H) stretch
-OH	m-s	3636	3666	ν(-OH) stretch

6. Thermogravimetric measurements

The thermogravimetric measurements were performed on a NETZSCH STA 409 CD analyzer (Airflow = 75 mL/min, heating rate = 4 K/min). The sample amount was approximately 30 mg for each sample. PXRD patterns collected after the measurement are shown below (Fig. S21) along with the plots of the thermogravimetric measurements (Fig. S22-27). PXRD analysis of the residues obtained from [Al(OH)(**1,8-ndc**)] and [$Al_2(OH)_4$(**2,3-ndc**)] after the TG measurements showed the formation of an amorphous decomposition product. Theoretical calculations were done assuming the residue was Al_2O_3.

The results of the evaluation of the TG curves is presented in the main manuscript.

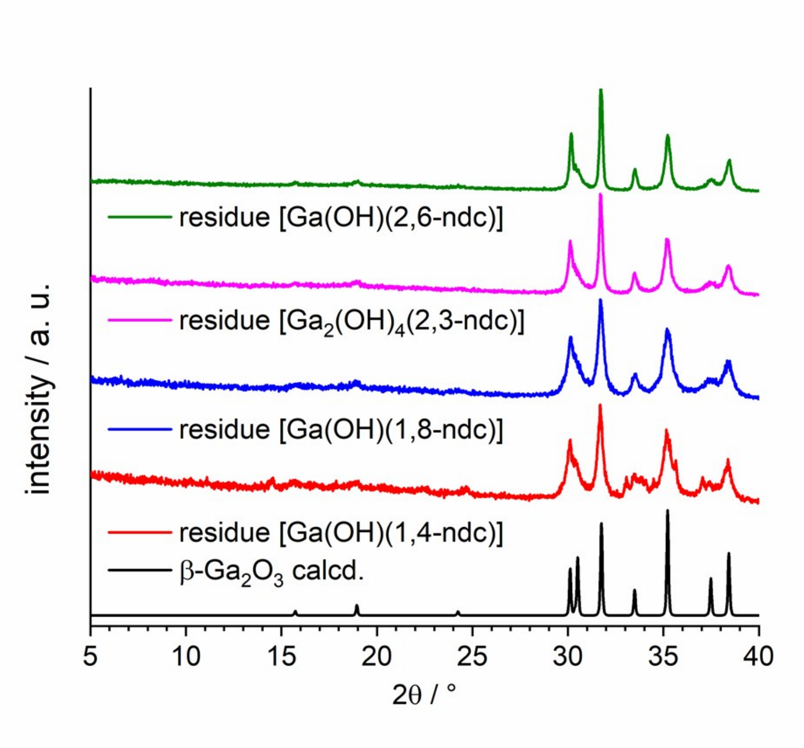

Figure S21: *PXRD pattern for each residue of the thermogravimetric measurement.*

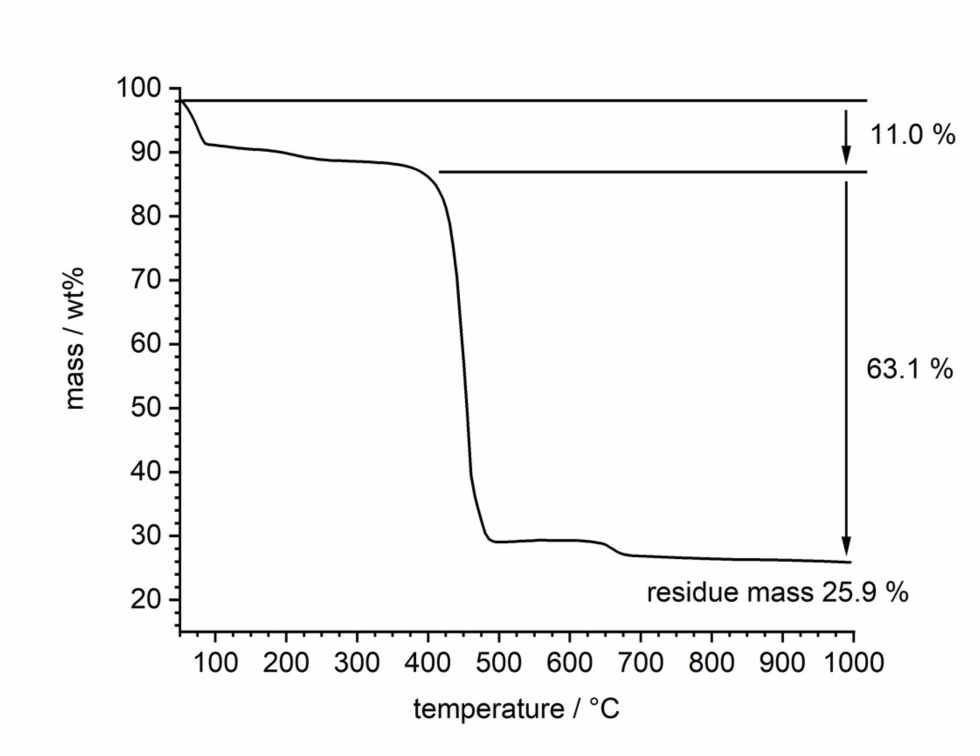

Figure S22: *Thermogravimetric curve of [Ga(OH)(**1,4-ndc**)].*

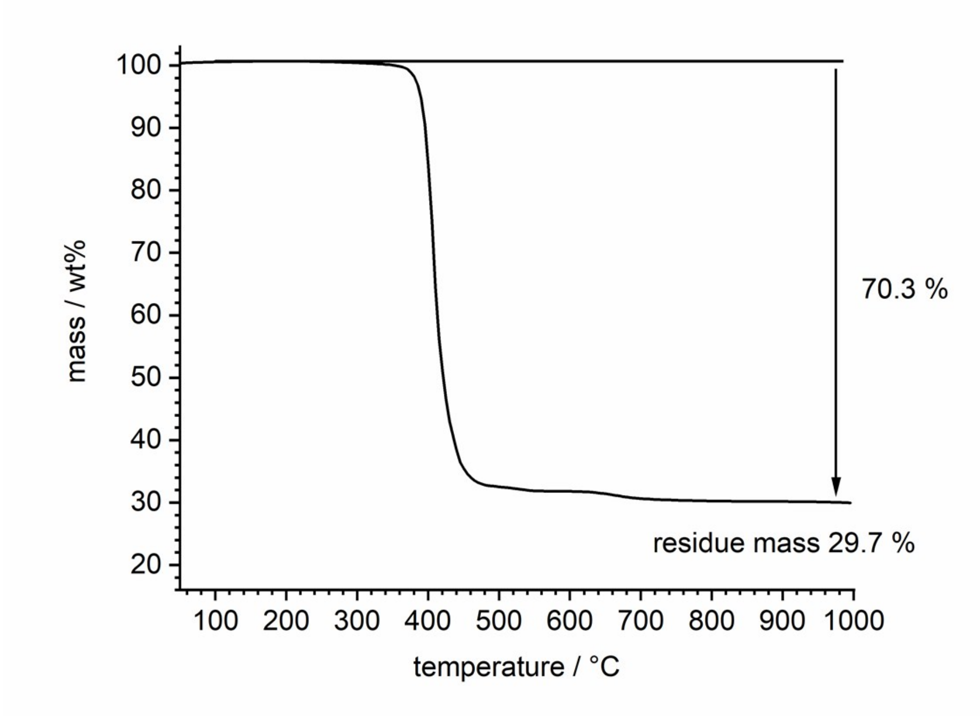

Figure S23: *Thermogravimetric curve of [Ga(OH)(**1,8-ndc**)].*

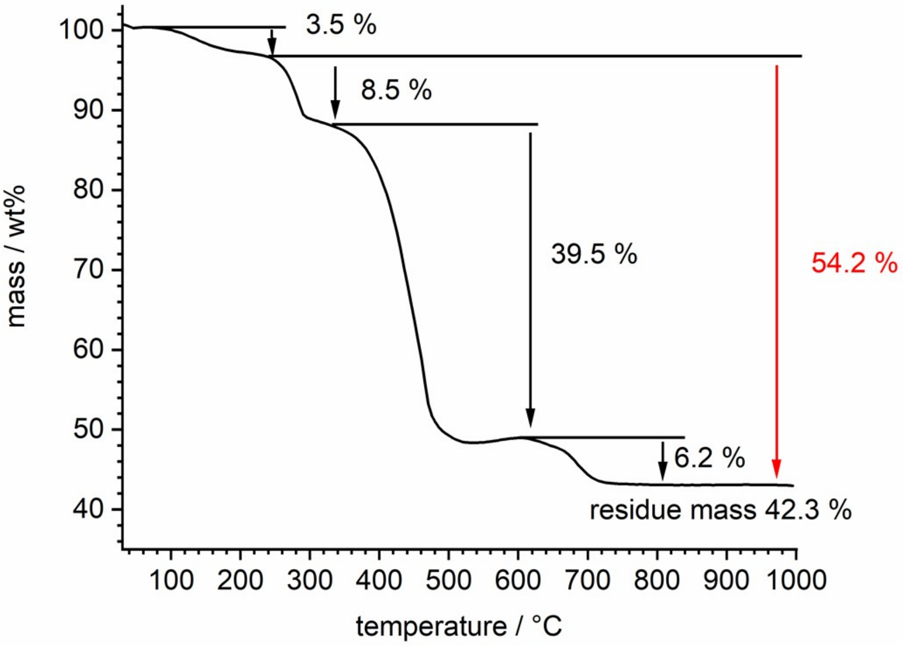

Figure S24: *Thermogravimetric curve of [Ga$_2$(OH)$_4$(**2,3-ndc**)].*

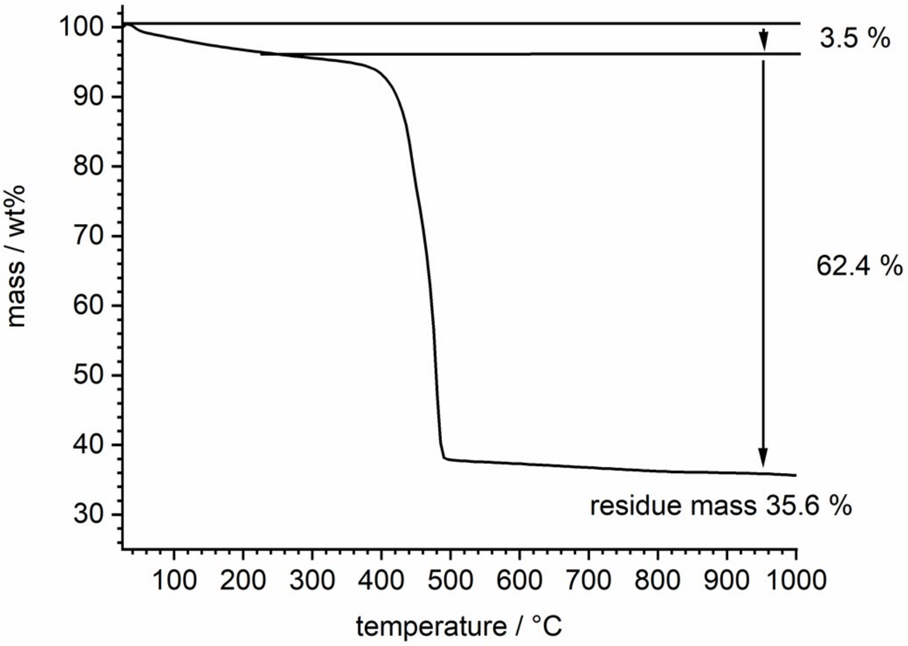

Figure S25: *Thermogravimetric curve of [Ga(OH)(**2,6-ndc**)].*

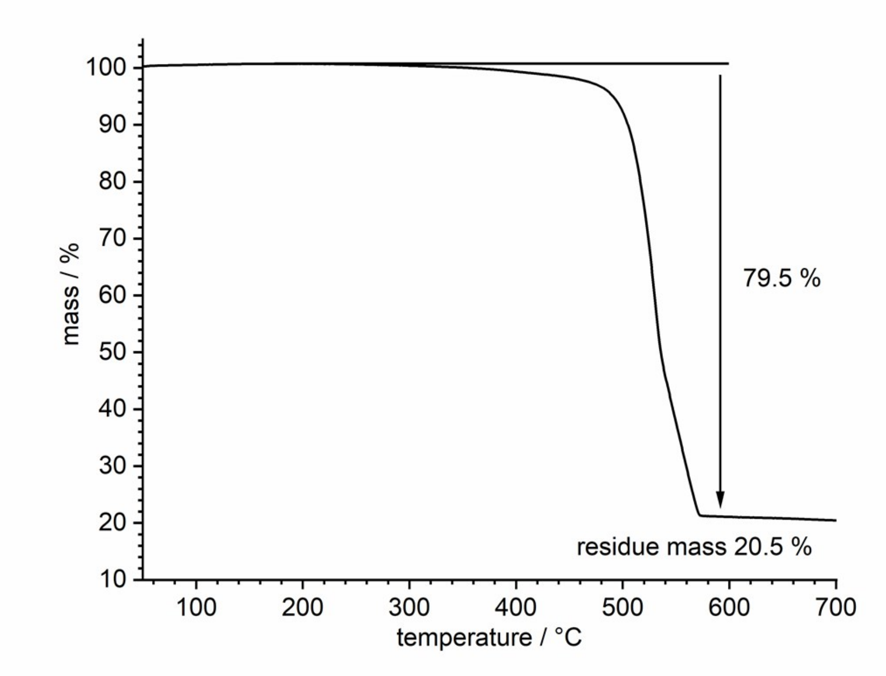

Figure S26: *Thermogravimetric curve of [Al(OH)(**1,8-ndc**)].*

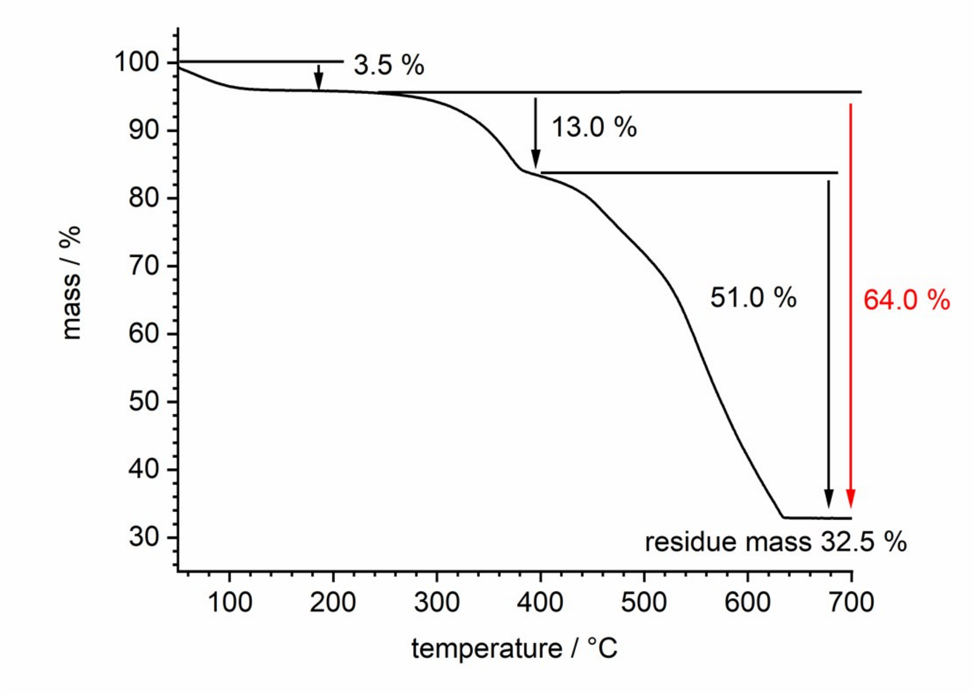

Figure S27: *Thermogravimetric curve of [$Al_2(OH)_4$(**2,3-ndc**)].*

7. Temperature dependent PXRD

Temperature dependent PXRD measurements are shown below (Fig. S28-33).

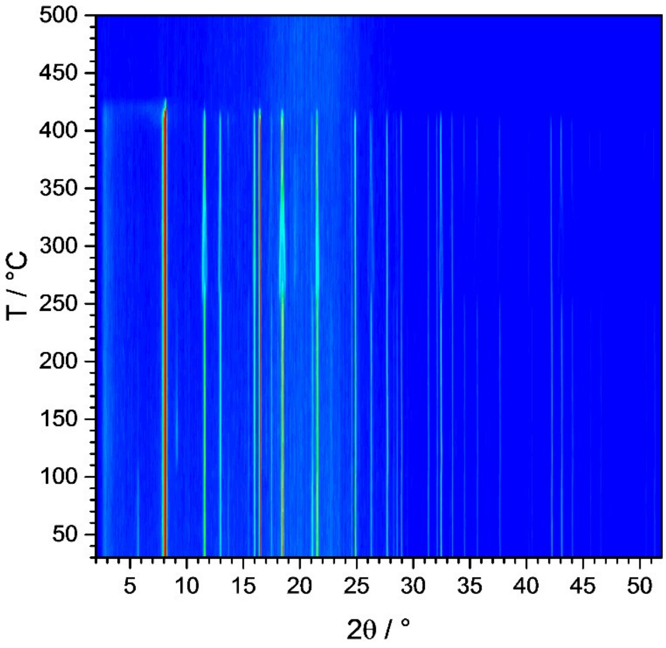

Figure S28: *Temperature dependent PXRD measurement of [Ga(OH)(**1,4-ndc**)].*

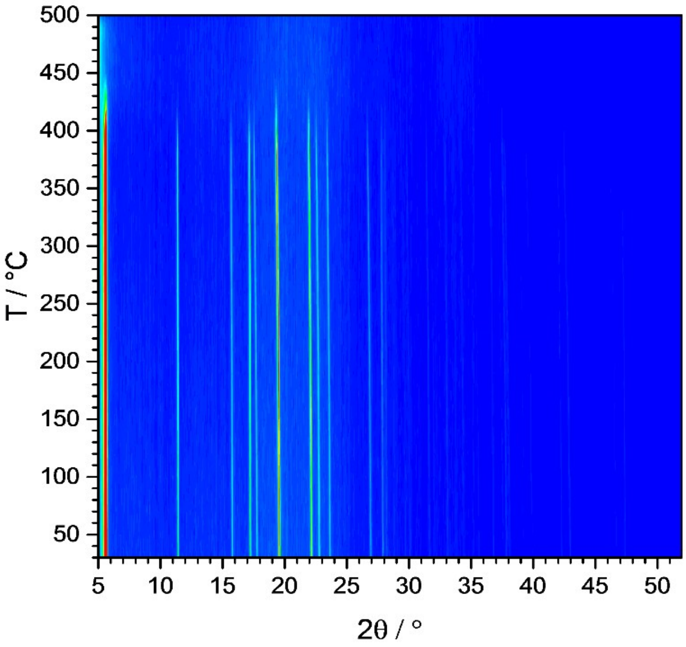

Figure S29: *Temperature dependent PXRD measurement of [Ga(OH)(**1,8-ndc**)].*

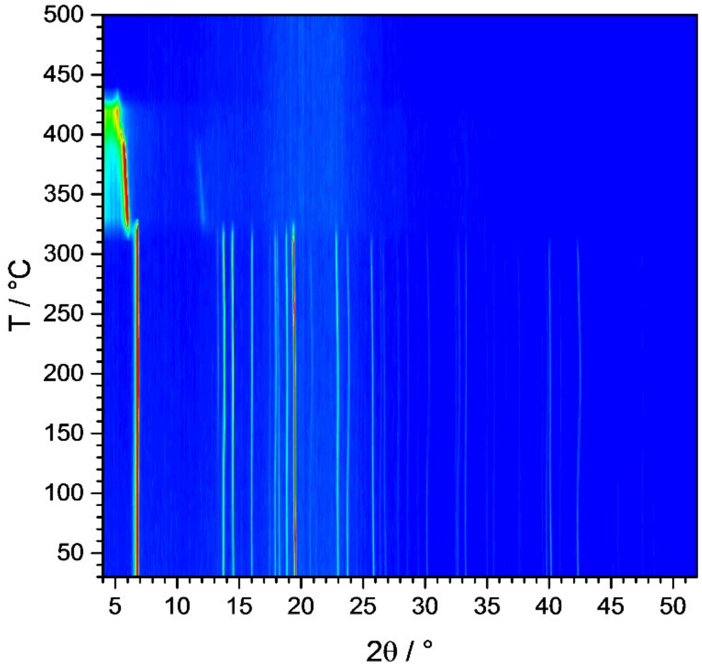

Figure S30: *Temperature dependent PXRD measurement of [$Ga_2(OH)_4$(**2,3-ndc**)].*

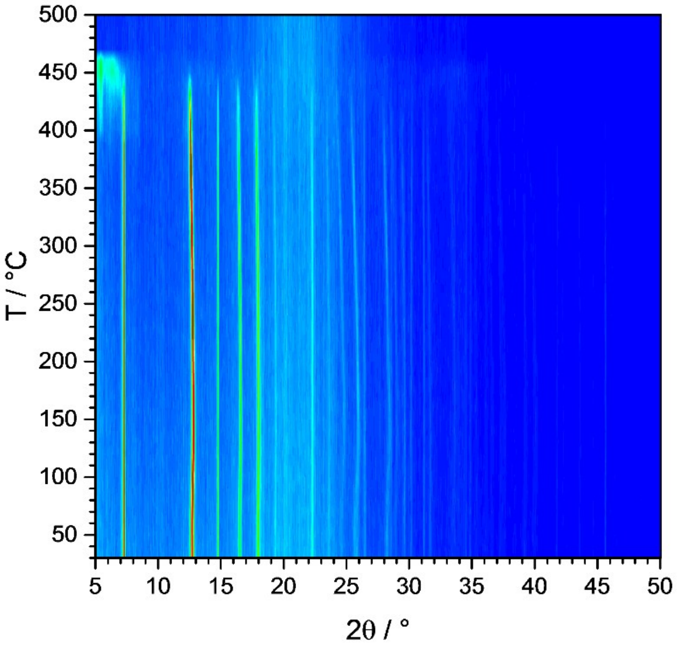

Figure S31: *Temperature dependent PXRD measurement of [Ga(OH)(**2,6-ndc**)].*

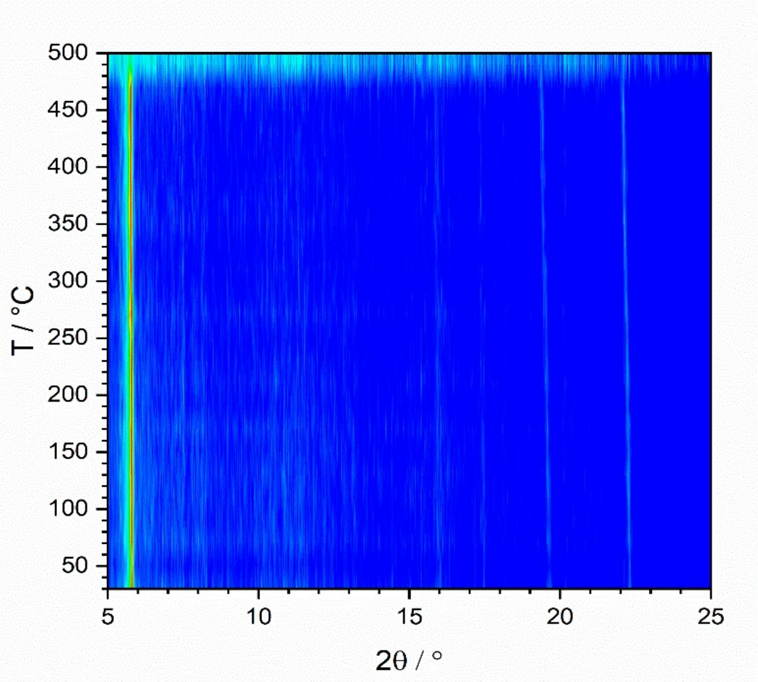

Figure S32: *Temperature dependent PXRD measurement of [Al(OH)(**1,8-ndc**)].*

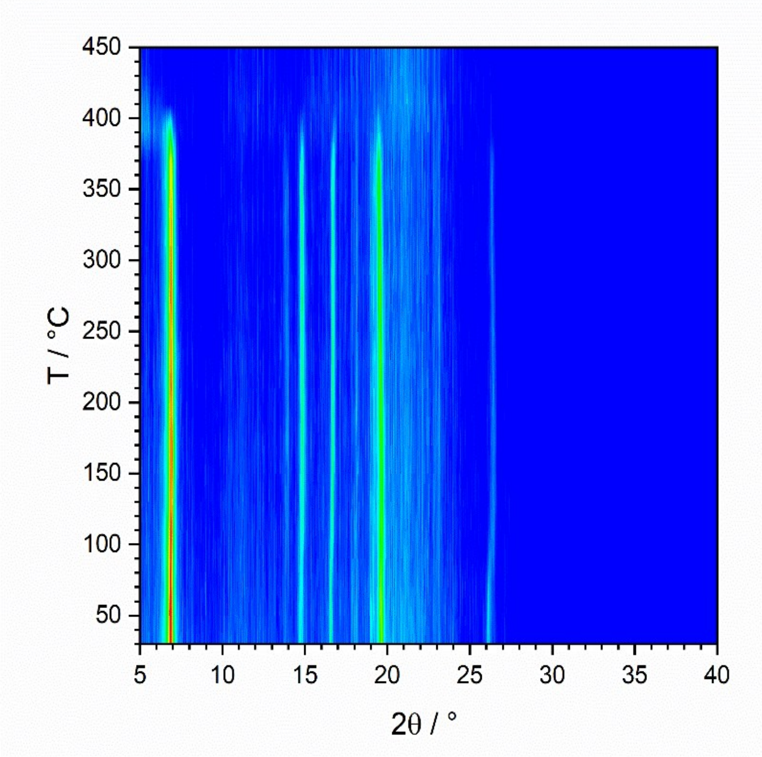

Figure S33: *Temperature dependent PXRD measurement of [$Al_2(OH)_4$(**2,3-ndc**)].*

Deviations of the decomposition temperatures obtained from temperature dependent PXRD measurements and thermogravimetric measurements can be explained through the different experimental setups. Whereas the thermogravimetric measurements are performed in a flow of air in Al_2O_3 crucibles, the temperature dependent PXRD measurements are carried out in densely packed 0.5 mm quartz capillaries, which can be considered as a more closed environment.

8. Sorption Isotherms

Nitrogen and water vapor sorption measurements are shown below (Fig. S34-42) as well as PXRD patterns collected before and after the activation (Fig. S43-48). The activation temperature and -time for all six title compounds are listed in Table S15.

Table S15: *Activation temperature and time for all title compounds. Activation was carried out under reduced pressure (dynamic vacuum, $p < 10^{-2}$ mbar).*

Compound	T / °C	t / h
[Ga(OH)(1,4-ndc)]	250	16 h
[Ga(OH)(1,8-ndc)]	180	16 h
[$Ga_2(OH)_4$(2,3-ndc)]	160	16 h
[Ga(OH)(2,6-ndc)]	180	16 h
[Al(OH)(1,8-ndc)]	180	16 h
[$Al_2(OH)_4$(2,3-ndc)]	180	16 h

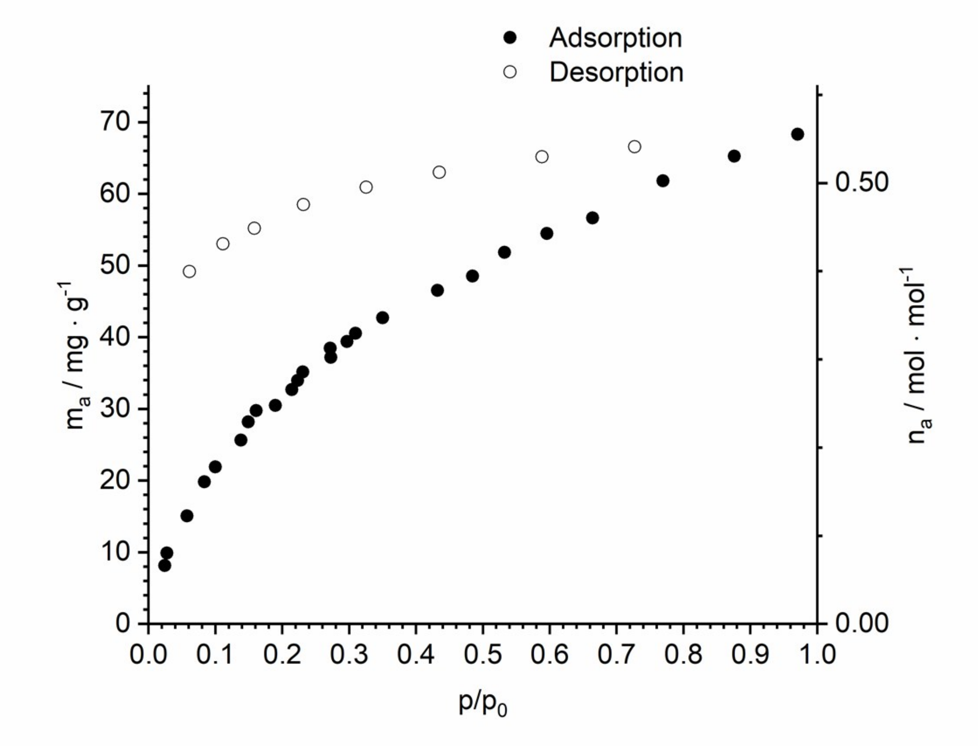

Figure S34: *Water vapor sorption isotherm of [$Ga_2(OH)_4$(**2,3-ndc**)].*

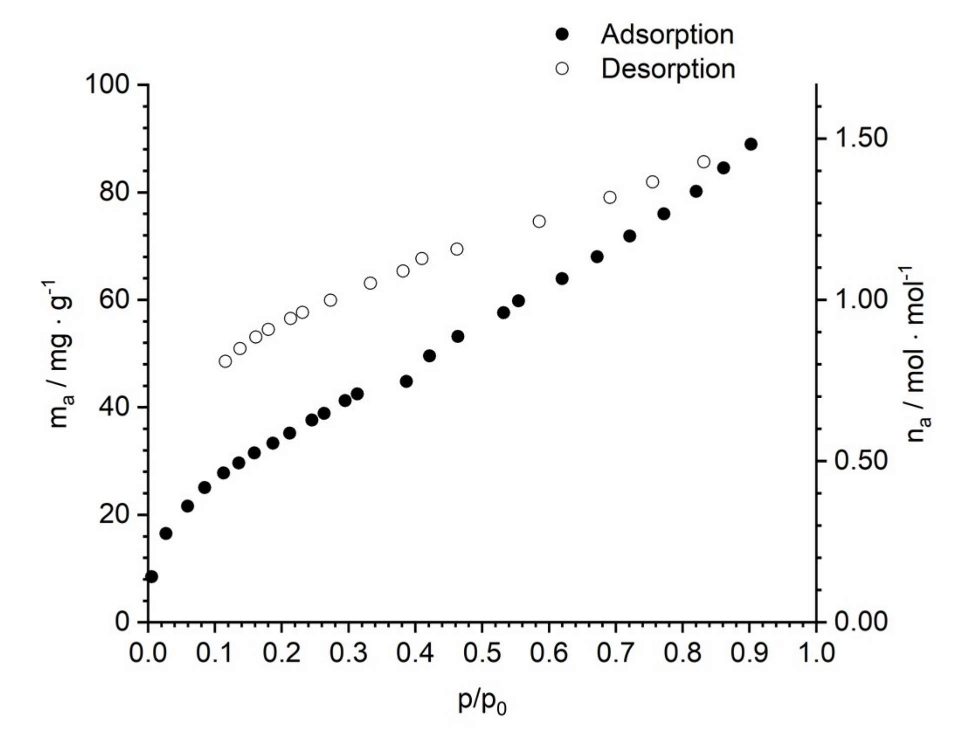

Figure S35: *Water vapor sorption isotherm of [Ga(OH)(**2,6-ndc**)].*

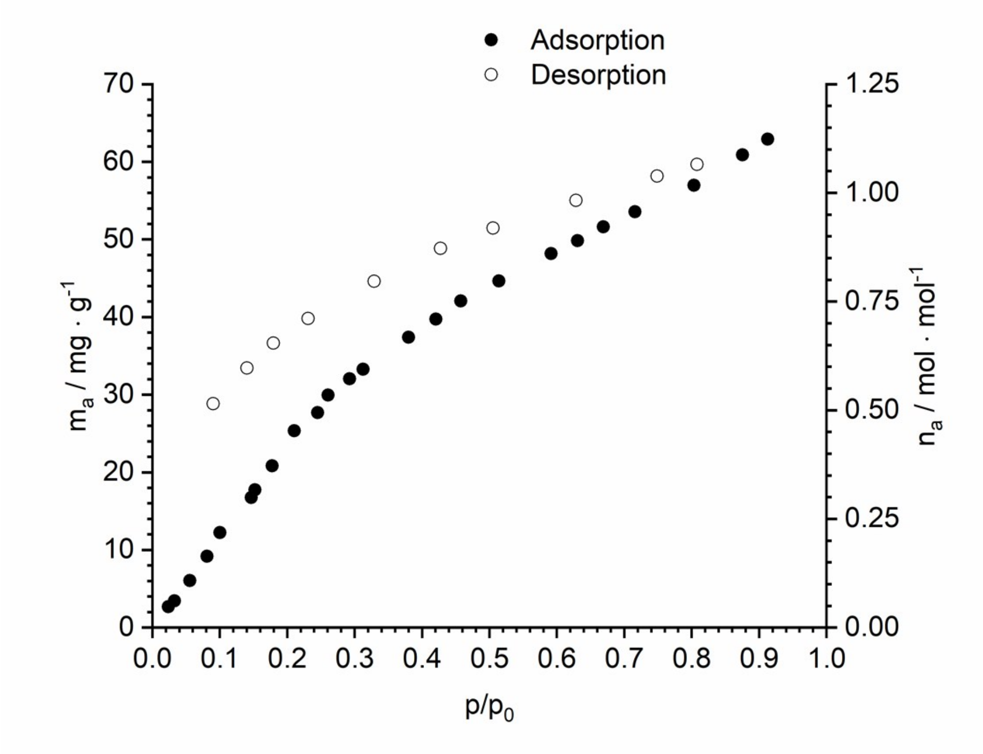

Figure S36: *Water vapor sorption isotherm of [Al$_2$(OH)$_4$(**2,3-ndc**)].*

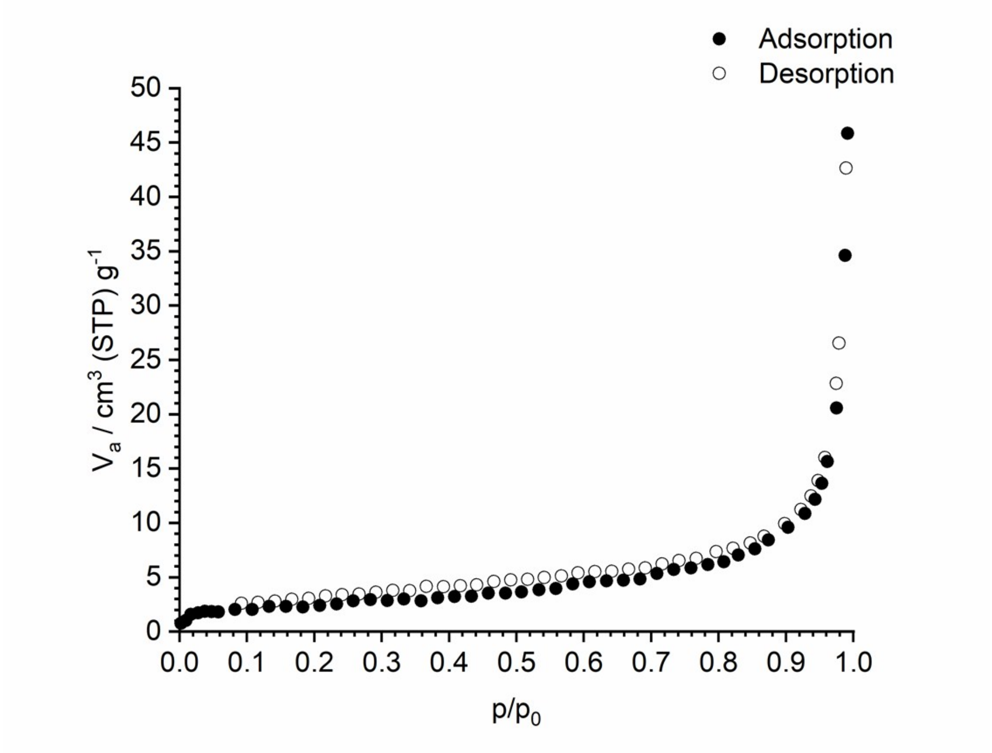

Figure S37: *Nitrogen sorption isotherm of [Ga(OH)(**1,4-ndc**)].*

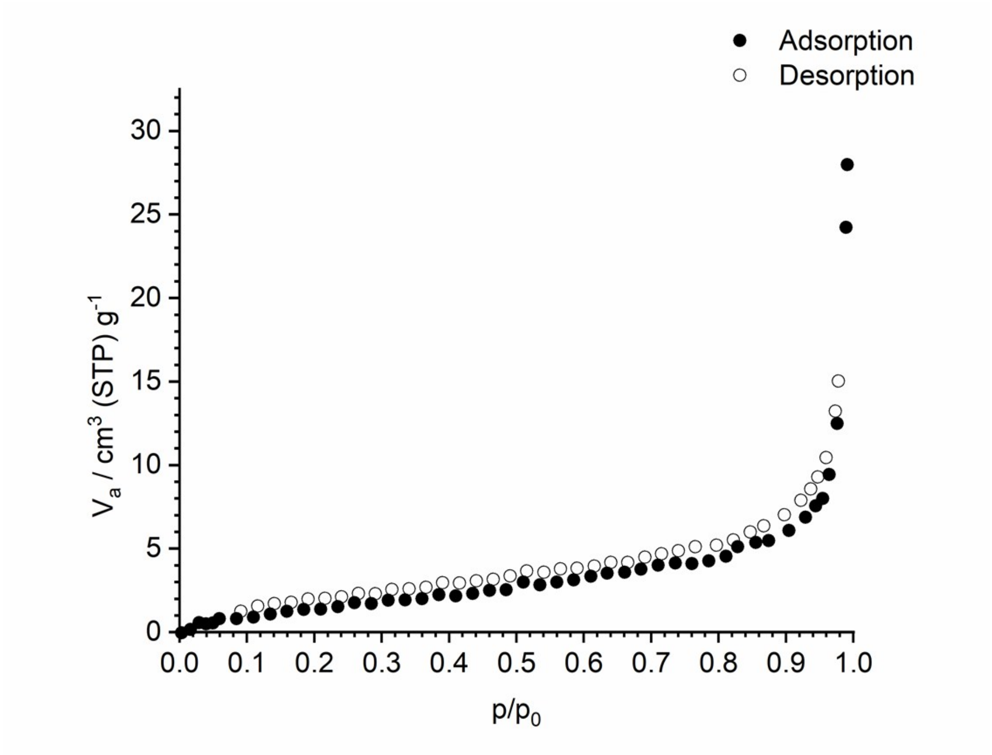

Figure S38: *Nitrogen sorption isotherm of [Ga(OH)(**1,8-ndc**)].*

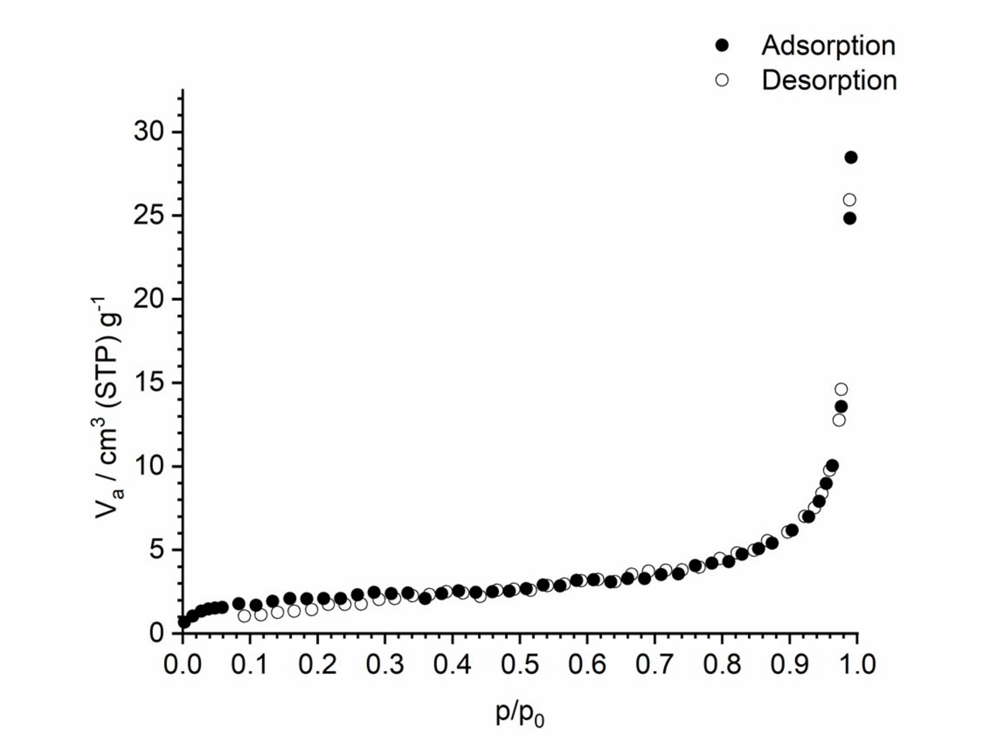

Figure S39: *Nitrogen sorption isotherm of [$Ga_2(OH)_4$(**2,3-ndc**)].*

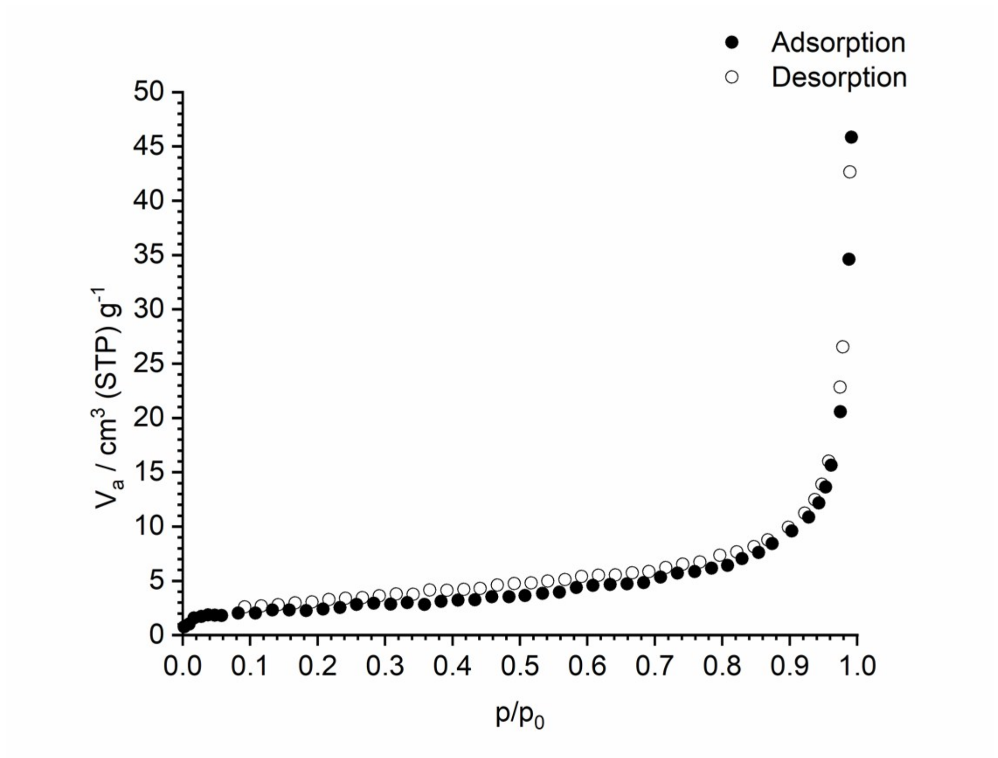

Figure S40: *Nitrogen sorption isotherm of [Ga(OH)(**2,6-ndc**)].*

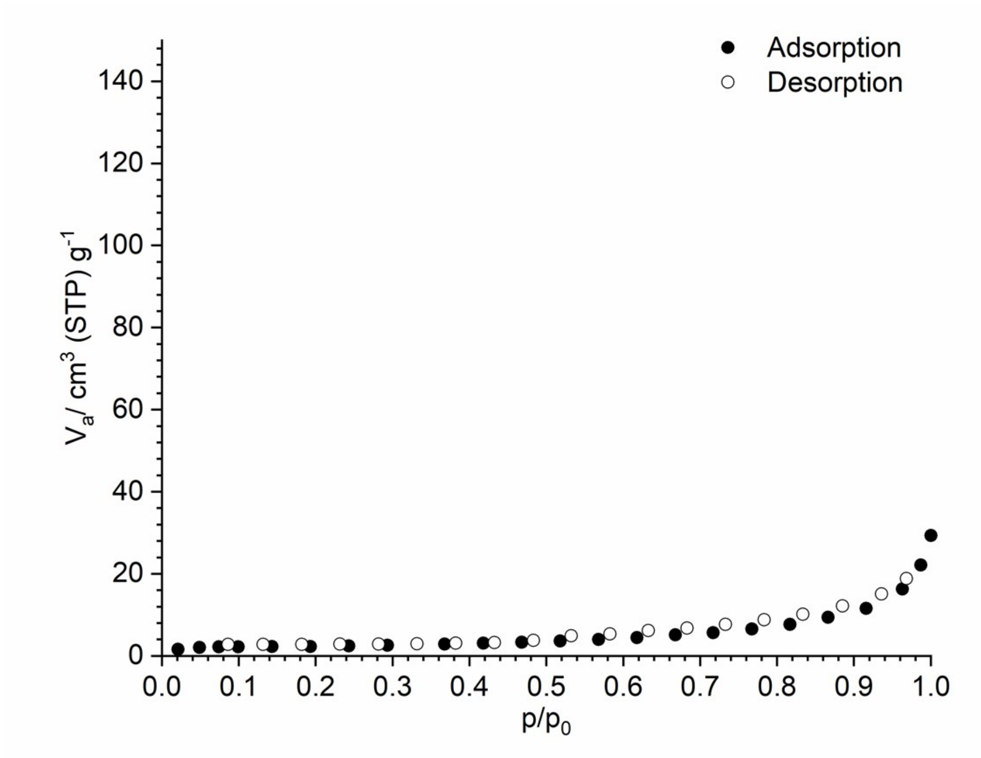

Figure S41: *Nitrogen sorption isotherm of [Al(OH)(**1,8-ndc**)].*

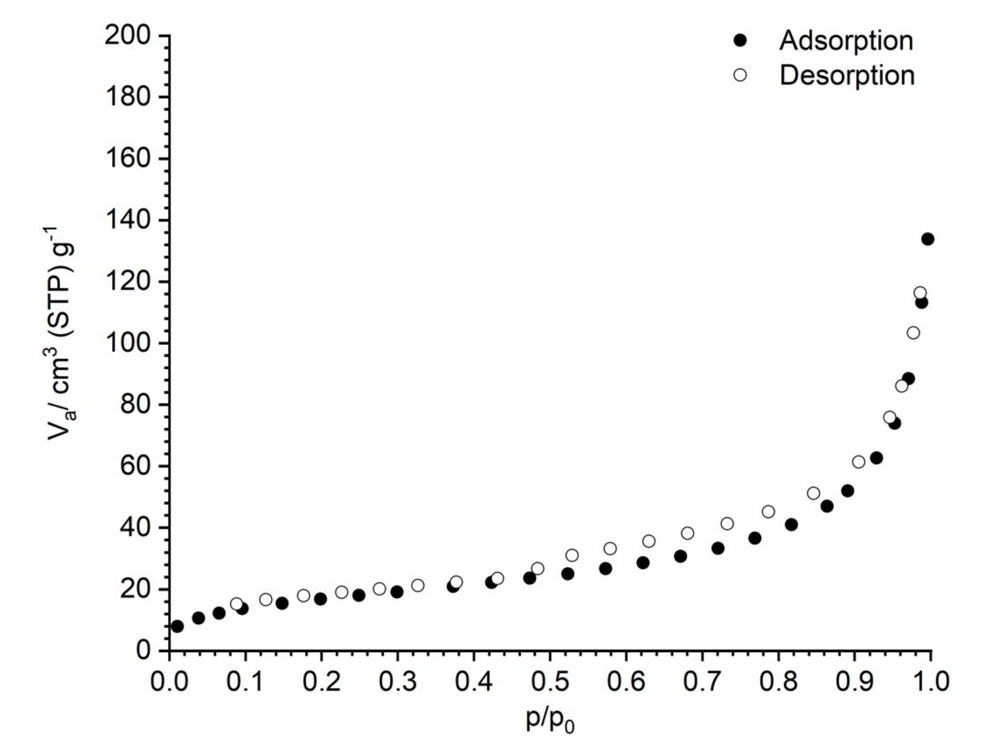

Figure S42: *Nitrogen sorption isotherm of [$Al_2(OH)_4$(**2,3-ndc**)].*

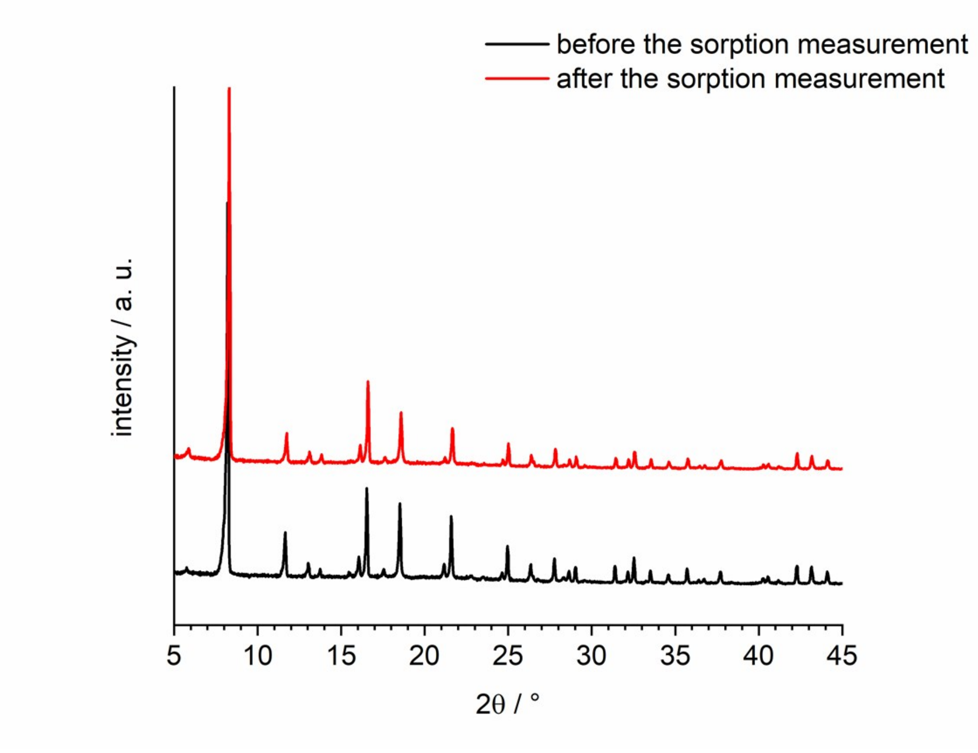

Figure S43: *PXRD pattern before and after the sorption measurement of [Ga(OH)(**1,4-ndc**)]. Activation was carried out under reduced pressure at 250 °C for 16 h.*

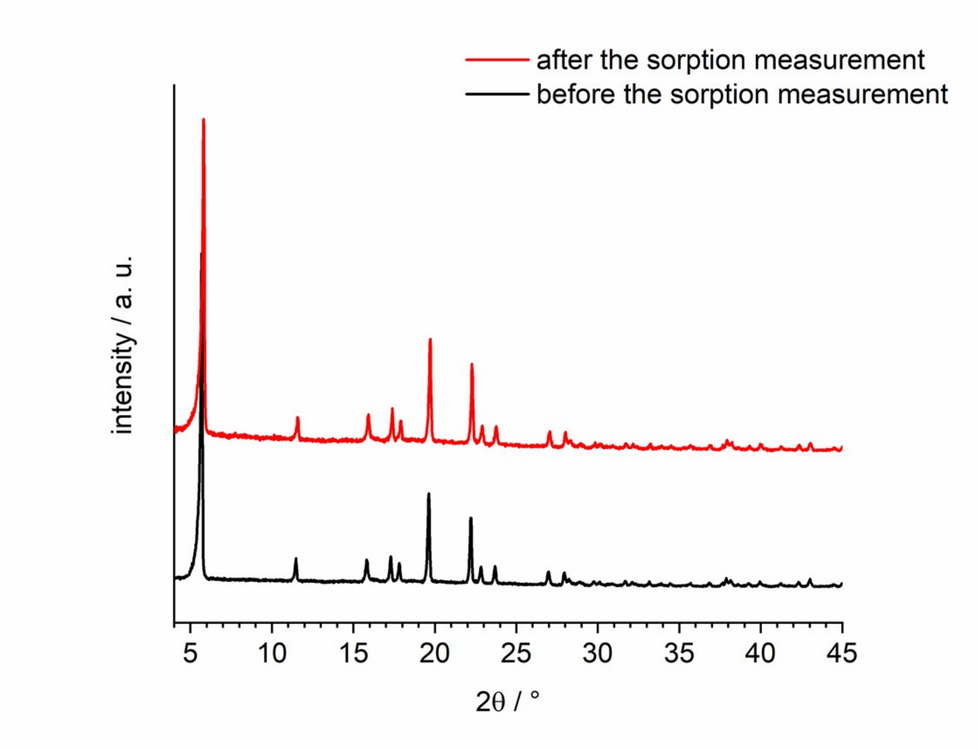

Figure S44: *PXRD pattern before and after the sorption measurement of [Ga(OH)(**1,8-ndc**)]. Activation was carried out under reduced pressure at 180 °C for 16 h.*

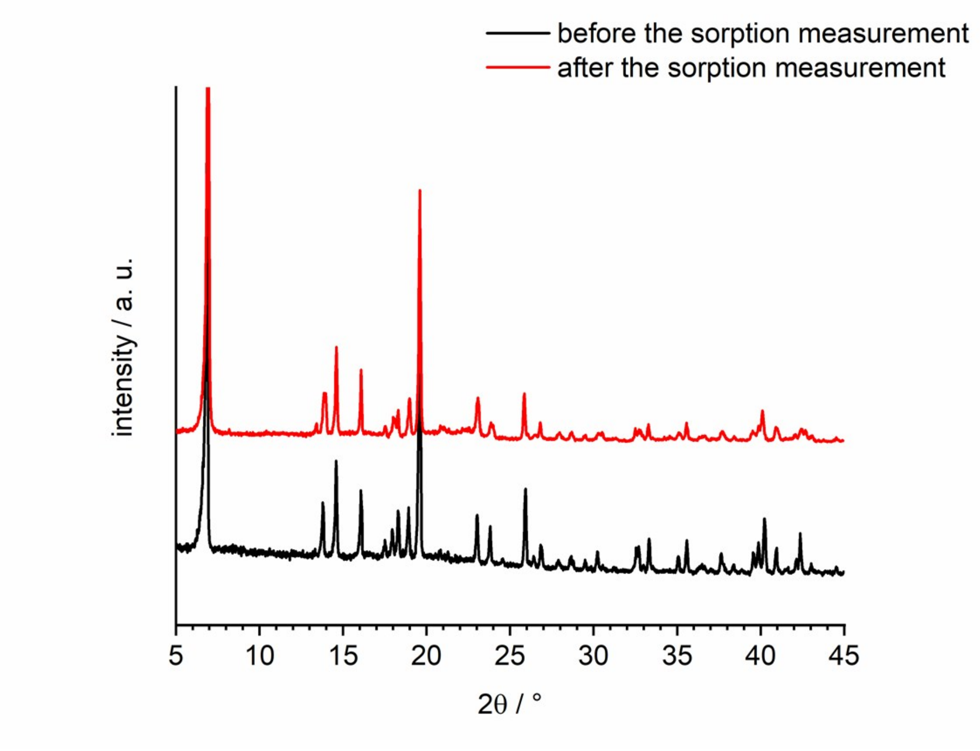

Figure S45: *PXRD pattern before and after the sorption measurement of [$Ga_2(OH)_4$(**2,3-ndc**)]. Activation was carried out under reduced pressure at 160 °C for 16 h.*

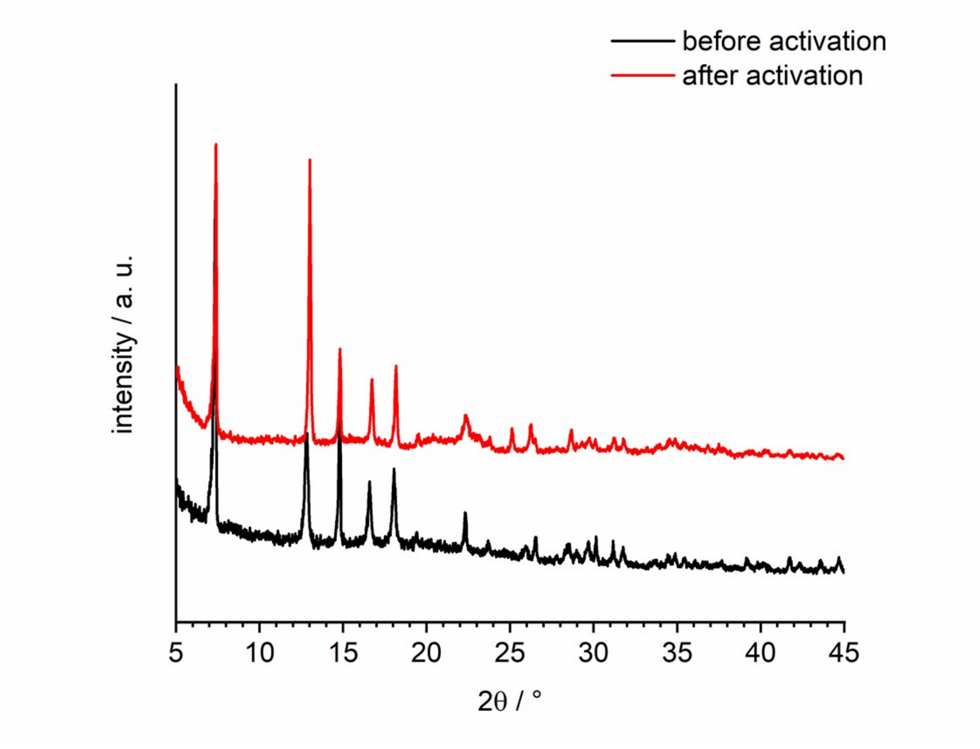

Figure S46: *PXRD pattern before and after the sorption measurement of [Ga(OH)(**2,6-ndc**)]. Activation was carried out under reduced pressure at 180 °C for 16 h.*

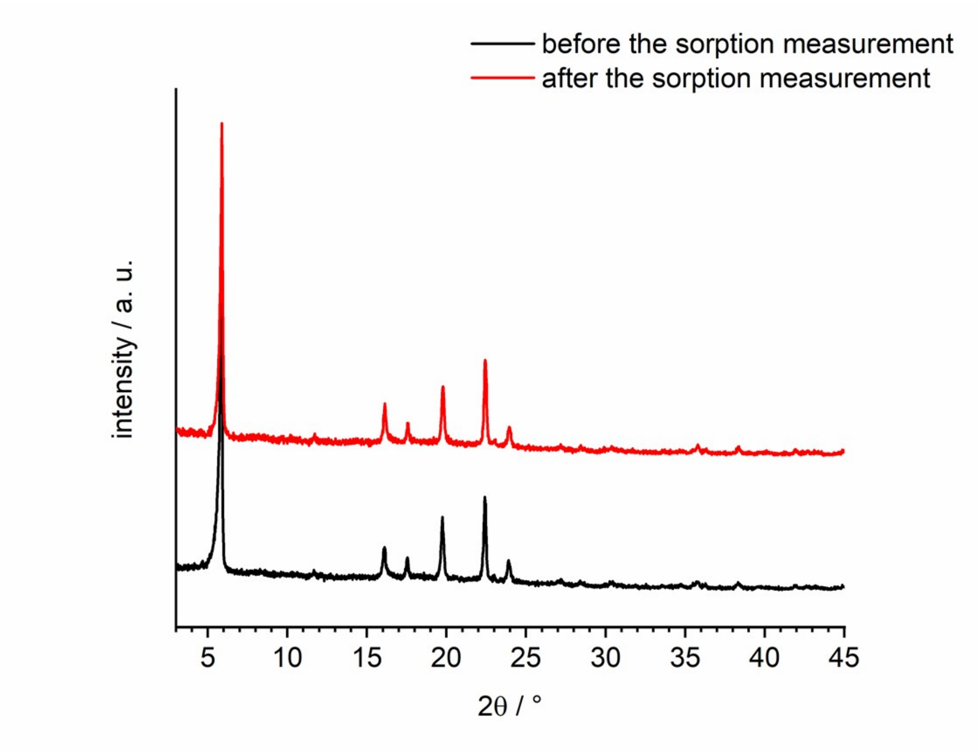

Figure S47: *PXRD pattern before and after the sorption measurement of [Al(OH)(**1,8-ndc**)]. Activation was carried out under reduced pressure at 180 °C for 16 h.*

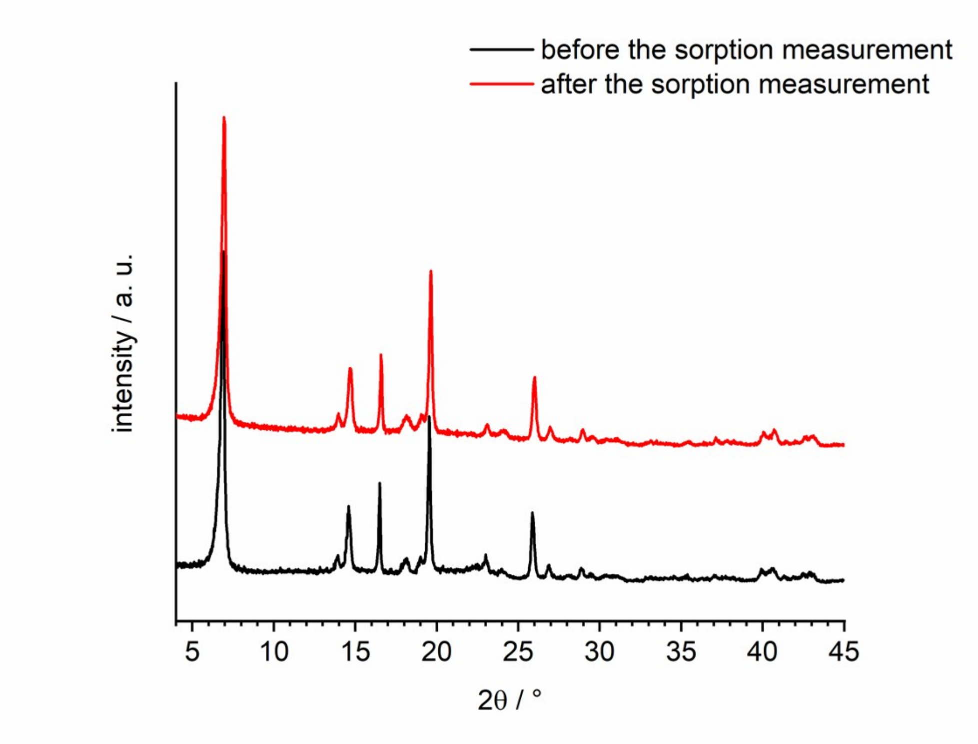

Figure S48: *PXRD pattern before and after the sorption measurement of [$Al_2(OH)_4$(**2,3-ndc**)]. Activation was carried out under reduced pressure at 180 °C for 16 h.*

9. References

1 M. O. Cichocka, J. Angstrom, B. Wang, X. Zou and S. Smeets, *J. Appl. Cryst.*, 2018, **51**, 1652–1661.

2 W. Kabsch, *Acta Cryst. D*, 2010, **66**, 125–132.

3 G. Sheldrick, *Acta Cryst. C*, 2015, **71**, 3–8.

4 G. Sheldrick, *Acta Cryst. A*, 2008, **64**, 112–122.

5 M. C. Burla, R. Caliandro, B. Carrozzini, G. L. Cascarano, C. Cuocci, C. Giacovazzo, M. Mallamo, A. Mazzone and G. Polidori, *J. Appl. Cryst.*, 2015, **48**, 306–309.

6 A. Coelho, *J. Appl. Cryst.*, 2018, **51**, 210–218.

7 Accelrys Incorporated, *Materials Studios*, San Diego, 2009.

8 X. Liu, G. Li, Y. Hu, M. Yang, X. Kong, Z. Shi and S. Feng, *Cryst. Growth Des.*, 2008, **8**, 2453–2457.

9 N. Heidenreich, A. Lieb, N. Stock and H. Reinsch, *Dalton Trans.,* 2018, **47**, 215–223.

10 T. Loiseau, C. Mellot-Draznieks, H. Muguerra, G. Férey, M. Haouas and F. Taulelle, *C. R. Chim.*, 2005, **8**, 765–772.

11 G. Socrates, *Infrared and Raman Characteristic Group Frequencies. Tables and Charts*, Wiley-VHC, Verlag GmbH & Co. KGaA, Weinheim, Germany, 2004.